Surveys in Geophysics (2021) 42:1075–1107
https://doi.org/10.1007/s10712-021-09652-6

The Global Water Cycle Budget: A Chronological Review

Mijael Rodrigo Vargas Godoy[1] · Yannis Markonis[1] · Martin Hanel[1] · Jan Kyselý[1,2] · Simon Michael Papalexiou[1,3,4]

Received: 11 November 2020 / Accepted: 30 June 2021 / Published online: 19 August 2021

Abstract
Like civilization and technology, our understanding of the global water cycle has been continuously evolving, and we have adapted our quantification methods to better exploit new technological resources. The accurate quantification of global water fluxes and storages is crucial in studying the global water cycle. These fluxes and storages physically interact with each other, are related through the water budget, and are constrained by it. First attempts to quantify them date back to the early 1900s, and during the past few decades, they have received an increasing research interest, which is reflected in the vast amount of data sources available nowadays. However, these data have not been comprehensive enough due to the high spatiotemporal variability of the global water cycle. Herein, we provide a comprehensive review of the chronological evolution of global water cycle quantification, the distinct data sources and methods used, and a critical assessment of their contribution to improving the spatiotemporal monitoring of the global water cycle. The chronology of global water cycle components shows that the uncertainty of flux estimates over oceans remains higher than that over land. Comparing the standard deviation and the interquartile range of the estimates from the 2000s onward with those from all the estimates (1905-2019), we can affirm that statistical variability has diminished in recent years. Moreover, the variability of ocean precipitation and evaporation estimates from the 2000 onward was reduced by more than 70% compared with earlier studies. These findings advocate that the consistency of global water cycle quantification has been improved.

Keywords Global water cycle · Water budget · Multi-source quantification

Abbreviations

CHIRPS	Climate Hazards Group Infrared Precipitation with Station Data
CLM3	Community Land Model version 3

✉ Mijael Rodrigo Vargas Godoy
vargas_godoy@fzp.czu.cz

[1] Faculty of Environmental Sciences, Czech University of Life Sciences Prague, Kamýcká 129, Praha – Suchdol 165 00, Czech Republic

[2] Institute of Atmospheric Physics, Czech Academy of Sciences, 14100 Prague 4, Czech Republic

[3] Department of Civil, Geological, and Environmental Engineering, University of Saskatchewan, Saskatoon, Saskatchewan S7N 5A9, Canada

[4] Global Institute for Water Security, Saskatoon, Saskatchewan S7N 3H5, Canada

CMORPH	Climate Prediction Center Morphing Method
CPC	Climate Prediction Center
CRU TS	University of East Anglia Climatic Research Unit Time-Series
CSR	Center for Space Research at University of Texas
CSU	Colorado State University
DMSP	Defense Meteorological Satellite Program
ECMWF	European Centre for Medium-Range Weather Forecasts
ERA	European Centre for Medium-Range Weather Forecasts Re-Analysis
GEWEX	Global Energy and Water Exchanges
GFZ	Deutschen GeoForschungsZentrum
GHP	Global Energy and Water Exchanges Hydrometeorology Panel
GLDAS	Global Land Data Assimilation System
GLEAM	Global Land Evaporation Amsterdam Model
GPCC	Global Precipitation Climatology Centre
GPCP	Global Precipitation Climatology Project
GPM	Global Precipitation Measurement
GRACE	Gravity Recovery and Climate Experiment
GRDC	Global Runoff Data Centre
GRGS	Groupe de Recherche de Géodésie Spatiale
GWAVA	Global Water Availability Assessment
H08	Hanasaki 2008
HTESSEL	Land Surface Hydrology Tiled European Centre for Medium-Range Weather Forecasts Scheme for Surface Exchanges Over Land
JPL	Jet Propulsion Laboratories
JULES	Joint UK Land Environment Simulator
LPJmL	Lund-Potsdam-Jena Managed Land
MacPDM	Macro-scale Probability-Distributed Moisture
MATSIRO	Minimal Advanced Treatments of Surface Interaction and Runoff
MERRA	Modern-Era Retrospective Analysis for Research and Applications
MPI-HM	Max Planck Institute - Hydrology Model
MOD16	Moderate Resolution Imaging Spectroradiometer Global Evapotranspiration Project
MODIS	Moderate Resolution Imaging Spectroradiometer
NRL	Naval Research Laboratory
NTSG	Numerical Terradynamic Simulation Group
Orchidee	Organising Carbon and Hydrology in Dynamic Ecosystems
PGF	Princeton Global Forcing
PREC/L	Precipitation Reconstruction Over Land
SRB-CFSR-SEBS	Surface Radiation Budget - Climate Forecast System Reanalysis - Surface Energy Balance System
SRB-CFSR-PM	Surface Radiation Budget - Climate Forecast System Reanalysis - Penman-Monteith
SRB-CFSR-PT	Surface Radiation Budget - Climate Forecast System Reanalysis - Priestly-Taylor
SRB-PGF-PM	Surface Radiation Budget - Princeton Global Forcing - Penman-Monteith
SSM/I	Special Sensor Microwave Imager
SSMIS	Special Sensor Microwave Imager Sounder

TMPA	Tropical Rainfall Measuring Mission Multi-satellite Precipitation Analysis
TRMM	Tropical Rainfall Measuring Mission
VIC	Variable Infiltration Capacity
WaterGAP	Water Global Assessment and Prognosis

Article Highlights

- Global water cycle estimates into the perspective of a century of scientific research
- Evolution of methods, observing systems, and models dealing with the global water cycle and water budgets
- Status quo of the global water cycle and its responses to global warming

1 Introduction

Water and its continuous circulation through its global cycle have played a fundamental role in sustaining life on Earth since its formation. The global water cycle is a complex phenomenon composed of several physicochemical processes such as condensation, evaporation, groundwater flow, infiltration, percolation, plant uptake, precipitation, runoff, sublimation, transpiration, and water vapor transport (Allan et al. 2020), coupled with anthropogenic interactions like water withdrawals and soil moisture use for livestock, crop irrigation, and forestry (Abbott et al. 2019). The longstanding representation of the global water cycle's conceptual model has been limited to three variables, namely precipitation, evaporation and runoff. Recently, this coarse representation has been partitioned to include the aforementioned sub-processes and their feedbacks. Our understanding of the global water cycle has been evolving over the years, and the methods we use to quantify hydrometeorological variables have adapted to exploit new technologies. Furthermore, the need to better estimate the components of the global water cycle has driven tailor-made technological developments as well (e.g., satellite instruments; Hildebrand et al. 2003; Levizzani and Cattani 2019).

Remote sensing data and model simulations complemented the traditional surface-based measurements and offered unprecedented coverage over previously inaccessible or unmonitored regions. Even though these advances provided vast data sources and aided to quantify water cycle components at multiple scales, their varying performances and uncertainties limit their applicability to global scale analyses (Brocca et al. 2019). Thus, the number of primary components used to quantify the global water cycle has not changed much. The most substantial differences that arose with the inclusion of satellite data are the decomposition of total evaporation into evaporation over oceans and evapotranspiration over land (Dickinson 1984), and the addition of total water storage (L'vovitch M, 1973). The above components represent the major inputs, outputs, and storage of the global water cycle. Hence, if we apply the mass conservation principle, we may write the water budget equation, which relates to these four components as follows.

$$\Delta \mathrm{TWS} = P - \mathrm{ET} - Q \quad (1)$$

where ΔTWS is the change in total water storage (as the sum of groundwater, soil moisture, and surface water such as river water, snow water, and water in lakes), P is precipitation, ET is evapotranspiration, and Q is the net water transport. The rest of the global water cycle processes are, to some extent, encompassed in these four components (Bengtsson 2010). Inadvertently, aggregating global water cycle components to the most dominant ones also aggregates the underlying uncertainties of the minor components, which are overshadowed by the uncertainties of the major components with the available accuracy at the moment. Global water cycle quantification accuracy is further hindered by the inherent biases revealed in the first attempts to unify multiple data sources for a single component due to the vast heterogeneity of algorithms and data used (Hegerl et al. 2018).

Uncertainties in the quantification of global water cycle components are indispensable when attempting to close the water budget. We can express equation 1 as:

$$P - \mathrm{ET} - Q - \Delta\mathrm{TWS} = R \tag{2}$$

where R is the budget residual, which in a closed budget equals to zero. Through the years, there have been various attempts to close the budget (Starr and Peixoto 1958; Willmott et al. 1985; Sheffield et al. 2009; Sahoo et al. 2011). They have used different data sources and methods to minimize the residual, but non-closure of the water budget still prevails. Alternatively, rather than using budget closure as the performance metric, some researchers prefer to look at runoff as a diagnostic flux to assess their results (Sheffield et al. 2009). Closing the water budget not only will improve our understanding of the global water cycle, but will necessarily lead to improvement of the accuracy of the data involved. Enhancing data accuracy is of critical importance for applications in climatology, hydrology, meteorology, and water resource management, to name a few.

To keep moving forward towards closure of the global water cycle, with more accurate data, it would be beneficial to assess previous achievements. Herein, we present a review of the chronological evolution of the paradigms regarding the global water cycle budget. We provide an in-depth recapitulation of the advancements in global water cycle quantification. In addition, we present a comparison between budgets reported in the literature, with highlights on the methods and data sources used. Using significant technological improvements as timeline reference milestones, we considered four epochs, namely Early Days of Hydrology, Model Simulations Period, Satellite Era, and Age of Big Data. Each epoch is characterized by its own accomplishments and challenges. Some of the latter were overcome in succeeding epochs and some prevailed up to the present. Despite data reaching unprecedented availability, detail, and coverage, the quest for robust quantification of the global water cycle remains.

2 Chronicle

2.1 Early Days of Hydrology

Studies of the global water cycle are as old as hydrology. In classical Greece, Plato and Aristotle philosophized that groundwater might be the component responsible for circulating water resources by connecting rivers and lakes. However, Marcus Vitruvius is most commonly credited to be the first one to conceptualize the water cycle. In the first century BCE, Vitruvius proposed a philosophical description of the water cycle that placed precipitation instead of groundwater as a critical component of water transport (Pollio 1648).

Vitruvius planted a seed that would later lead both, yet independently, during the sixteenth century, Leonardo da Vinci and Bernard Palissy into describing a water cycle with three principal components: precipitation, evaporation, and runoff (Palissy 1580; Pfister et al. 2009). Therefore, equation 1 was originally formulated as:

$$P - E = Q \tag{3}$$

where P is precipitation, E is evaporation, and Q is the runoff or exceeding precipitation. With this theoretical formulation, the scientific community ventured into quantifying the above components during the seventeenth century. Pierre Perrault and Edmund Halley were among the pioneers that supplemented experimental science to hydrology with their research on catchment precipitation and evaporation, respectively (Brutsaert 2005). John Dalton was the first to quantify all three above-listed components for England and Wales, providing a comprehensive quantification of a water cycle and not just a single component of it (Dalton 1799).

With catchment scale quantification achieved, the next step was to aim for global-scale quantification. During the next years and up to the end of the 1960s, numerous studies, mainly coming from Germany and Russia, attempted to quantify the global water cycle. Baumgartner and Reichel (1972) surveyed the literature on global water cycle

Table 1 Modified from Baumgartner and Reichel (1972) to exclude incomplete rows

Author	P_L	ET	Q	P_O	E	P_{TOT}	E_{TOT}
Brückner (1905)	122	97	25	359	384	481	481
Fritzsche (1906)	112	81	31	353	384	465	465
Schmidt (1915)	112	81	31	242	273	354	354
Wüst (1922)	112	75	37	267	304	379	379
Cherubim (1931)	112	75	37	334	371	446	446
Meinardus (1934)	99	62	37	412	449	511	511
Halbfaß (1934)	100	52	48	410	458	510	510
Wüst and Defant (1936)	99	62	37	297	334	396	396
Wundt (1938)	99	62	37	346	383	445	445
L’vovitch M, (1945)	107	71	36	412	448	519	519
Möller (1951)	99	62	37	≤324	≤361	≤423	≤423
Reichel (1952)	100	70	30	315	345	415	415
Wüst et al. (1954)	100	73	27	324	351	424	424
Budyko (1955)	100	66	34-38	370	408	470	474
Albrecht (1960)	100	67	33	378	411	478	478
Budyko (1963)	107	61	46-48	404	452	512	513
Mira (1964)	108	72	36	412	448	520	520
Nace (1968)	100	69	31	319	350	419	419
Kessler (1968)	100	60	40	410	450	510	510
Mather (1969)	106	69	37	382	419	488	488
L’vovitch (1970)	109	72	37	411	448	520	520
Budyko (1970)	107	64	43	412	455	519	519

All the fluxes are in 10^3 km^3/year. P_L is precipitation overland, ET is evapotranspiration overland, Q is runoff, P_O is precipitation over oceans, E is evaporation over oceans, P_{TOT} is total global precipitation, and E_{TOT} is total global evaporation quantification during the 1900s and added their findings to the previous compilation by Reichel (1952), accounting for over 40 studies (Table 1). Over land, precipitation, range between (99 to 122) × 10^3 km^3/year, evapotranspiration range between (52 to 97) × 10^3 km^3/year, and runoff range between (25 to 48) × 10^3 km^3/year. Over oceans, precipitation and evaporation range between (242 to 412) × 10^3 km^3/year and (273 to 458) × 10^3 km^3/year, respectively. Note that evaporation and evapotranspiration have the most extensive ranges, presumably, because these values were derived from other measurements since, at the time, it was not possible to obtain direct observations. Even so, several reported fluxes are similar, if not identical, which may be caused by the fact that despite using different approximations or formulations, the initial data set used was the same. Over land precipitation estimates were derived from gauge and chart data, runoff estimates were derived from the river measurements by Marcinek (1964), and evaporation estimates were computed as the difference between precipitation and runoff. Over oceans, heat balance maps, and climatological data for fixed locations constituted evaporation estimates, runoff is the same as overland because of atmospheric water balance (Rasmussen 1970), and precipitation estimates were the difference between evaporation and runoff.

Due to the high variability in time and space of global water cycle components, ground station reports were not representative of the surrounding areas. Besides, it has been typical for developing countries not to possess a ground station network dense enough to monitor global water cycle components in those regions (Willmott et al. 1994). Aware of the above, Baumgartner and Reichel (1972) introduced very strong yet somewhat arbitrary correction assumptions, and estimated the errors based on the biggest difference between the values compiled on their survey. Considering that the precipitation measured by rain gauges is smaller than the amount reaching the surface and there are different zonal climatic conditions overland, the authors suggest three different options to correct precipitation underestimation. They pointed out that the scenario selected is the most probable, yet no explanation is provided towards why that is. Correcting precipitation overland has a ripple effect because it is used to compute runoff, which is then used to compute precipitation over the oceans. Based on their assumptions, they report the quantification of the global water cycle had been achieved within a margin of ten percent relative error.

A decade later, Willmott et al. (1985) presented the first study with sufficient spatial coverage. Their study was based on temperature and precipitation observational data records from 13,332 globally distributed stations, and estimated terrestrial snow-cover, soil moisture, and evapotranspiration. Their work extended on previous regional studies over Africa (Mather 1962), Asia excluding U.S.S.R. (Mather 1963a), U.S.S.R. (Mather 1963b), Australia, New Zealand, and Oceania (Mather 1963c), Europe (Mather 1964a), North America excluding USA (Mather 1964b), USA (Mather 1964c), and South America (Mather 1965). The above cumulatively used only 8,565 stations from the same network Willmott et al. (1985) used on their study. Still, they had to use empirical equations and a revised version of the potential evapotranspiration method of Thornthwaite (1948) in order to derive snow-cover, soil moisture, and evapotranspiration from the temperature and precipitation observational data available. Willmott et al. (1985) did not report single values as annual averages, but presented their results in maps where it could be seen that annual mean evapotranspiration is approximately 173 × 10^3 km^3/year over continental regions near the equator, 43 × 10^3 km^3/year towards the poles, and below 43 × 10^3 km^3/year across the Sahara, Arabia and Central Asia. Nonetheless, we know now, technological limitations and the lack of data sources place the findings of the above discussed studies in a best-guess scenario only.

2.2 Model Simulations Period

In simple terms, General Circulation Models (GCMs) are a set of theoretical and empirical mathematical expressions that attempt to simulate climate's physical processes. They could be an atmospheric GCM, an oceanic GCM, or a coupled GCM. The first atmospheric GCM was introduced by Norman Phillips (1956), and it opened the door to new opportunities for global water cycle quantification (McGuffie and Henderson-Sellers 2001). Not long after, towards the end of the 1960s, the National Oceanic and Atmospheric Administration Geophysical Fluid Dynamics Laboratory developed the first coupled GCM (Manabe 1969). The basic structure of a GCM can be seen in Fig. 1. The GCM spatial domain is composed of 3D cells, whose horizontal grid is typically formed by latitude and longitude, and pressure levels determine the cell height. The number of physical processes considered and the complexity to which they are represented have continuously improved since the introduction of GCMs. Today's models further account for terrestrial vegetation and the carbon cycle with an explicit representation of biogeochemical processes—such models are referred to as Earth System Models or ESMs (Flato 2011; Collins et al. 2013; Hurrell et al. 2013; Flato et al. 2014; Otto-Bliesner et al. 2016).

Model simulations were initially driven exclusively by ground observations. Later on, satellite remote sensing, model reanalysis data sets, or different combinations of them were assimilated. Hydrological models revolutionized the quantification of the global water cycle by providing regular gridded data with global coverage as well as constant time steps. On top of that, both statistical and dynamical downscaling of GCMs and ESMs have evolved over the past decades to enable more reliable estimates (Tapiador et al. 2020). For example, the most recent release of the European Centre for Medium Range Weather Forecasts Reanalysis product (ERA-5), which is a reanalysis based on the European Centre for Medium-Range Weather Forecasts' Integrated Forecasting System (ECMWF's IFS) weather model, provides a 30 km global coverage with 137 atmospheric pressure levels

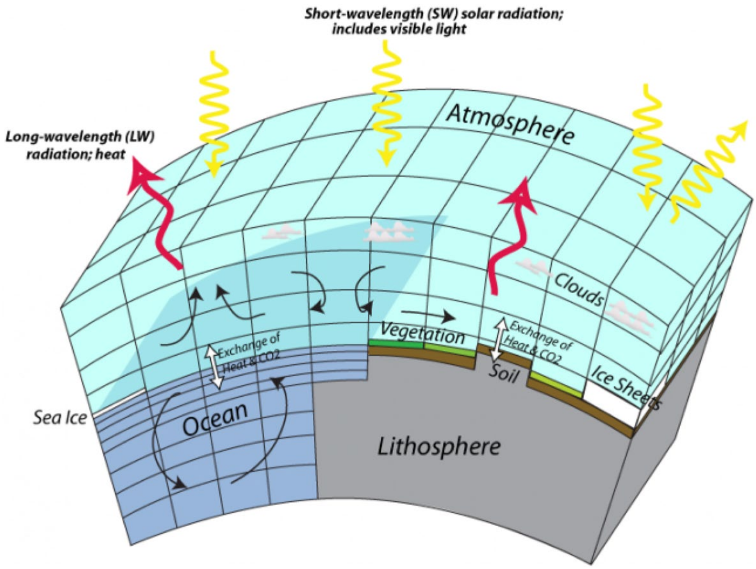

Fig. 1 Schematic structure of a General Circulation Model modified from Bralower and Bice (2012)

capped at 80 km with uncertainty ranges reported at each level (Hersbach et al. 2020). Despite the exponential growth in computing power efficiency, many fundamental processes like radiative transfer, convection initiation, hydrometeor phase change, and cloud microphysics that occur between the sub-kilometer scale and the microscale (i.e., nine orders of magnitude less than current model resolutions) are parameterized, as they cannot be resolved at the model resolution. On that account, while GCMs and ESMs provide global coverage of water cycle components, their spatial and temporal resolution is still relatively coarse, hindering validation attempts.

Model simulations further changed global water cycle quantification by providing more robust formulations towards the estimation of evapotranspiration. The bucket model developed by Budyko (1961) was implemented for the evapotranspiration scheme used in the first coupled GCM (Manabe 1969). This scheme oversimplified the physical processes surrounding evapotranspiration (Fig. 2); nevertheless, its results were not significantly different from much more complex formulations attempted in contemporaneous GCMs (Carson 1982). In the aforementioned scheme, evapotranspiration depends on potential evaporation, soil water content, field capacity (defined as the amount of soil moisture or water content held in the soil after excess water has drained away and the rate of downward movement has decreased), and water holding capacity (Carson 1982). Federer et al. (1996) compared five surface-independent and four surface-dependent potential evapotranspiration approximation schemes in models, and their results suggest that, at that time, none of the methods significantly differ from each other for most surface types. Still, the authors point out that the Penman-Monteith (Monteith and Unsworth 2013) and Shuttleworth & Wallace (Shuttleworth and Wallace 1985) methods might pose as the most comprehensive for global-scale analysis, a hypothesis that was later confirmed for Penman-Monteith (Wang and Dickinson 2012).

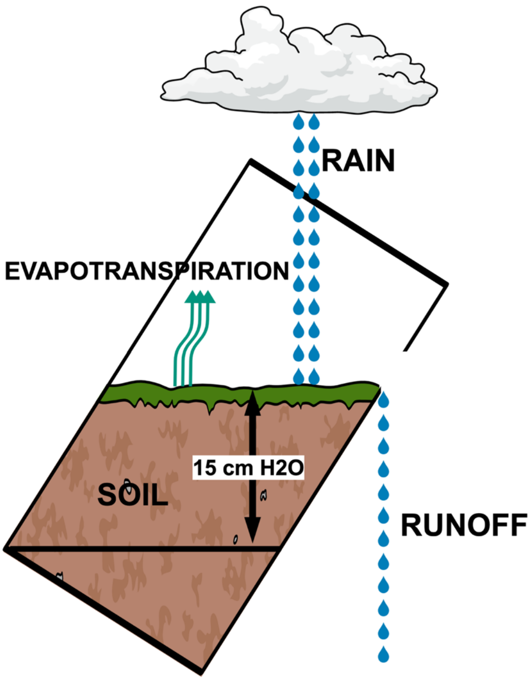

Fig. 2 Schematic of the Budyko bucket model implemented by Manabe (1969). The model represents a single layer soil reservoir with a defined maximum field water capacity of 15 cm from which soil water evaporates at a rate proportional to the remaining water content

Table 2 Modified from Haddeland et al. (2011)

Model name	Model time step	Meteorological forcing variables	ET scheme	Reference(s)
GWAVA	Daily	P, T, W, q, LW_{net}, SW, SP	Penman-Monteith	Meigh et al. (1999)
H08	6h	RR, S, T, W, q, LW, SW, SP	Bulk formula	Hanasaki et al. (2008)
HTESSEL	1h	RR, S, T, W, q, LW, SW, SP	Penman-Monteith	Balsamo et al. (2009)
JULES	1h	RR, S, T, W, q, LW, SW, SP	Penman-Monteith	Cox et al. (1999), Essery et al. (2003)
LPJmL	Daily	P, T, LW_{net}, SW	Priestley-Taylor	Bondeau et al. (2007), Rost et al. (2008)
MacPDM	Daily	P, T, W, q, LW_{net}, SW	Penman-Monteith	Arnell(1999), Gosling and Arnell (2011)
MATSIRO	1h	RR, S, T, W, q, LW, SW, SP	Bulk formula	Takata et al. (2003), Koirala (2010)
MPI-HM	Daily	P, T	Thornthwaite	Hagemann and Dümenil (1997), Hagemann and Gates (2003)
Orchidee	15 min	RR, S, T, W, q, SW, LW, SP	Bulk formula	de Rosnay and Polcher (1998)
VIC	Daily/3h	P, T_{max}, T_{min}, W, q, LW, SW, SP	Penman-Monteith	Liang et al. (1994)
WaterGAP	Daily	P, T, LW_{net}, SW	Priestley-Taylor	Alcamo et al. (2003)

LW is downward longwave radiation flux, LW_{net} is net longwave radiation flux, P is precipitation (rain or snow distinguished in the model), q is specific humidity, RR is rainfall rate, S is snowfall rate, SW is downward shortwave radiation flux, SP is surface pressure, T is air temperature, T_{max} is maximum daily air temperature, T_{min} is minimum daily air temperature, and W is wind speed. Bulk formula: Bulk transfer coefficients are used when calculating the turbulent heat fluxes

The coupled GCM introduced by Manabe (1969) simulated average values of 93.4 × 10^3 km^3/year overland precipitation, 69.5 × 10^3 km^3/year evapotranspiration, 23.9 × 10^3 km^3/year runoff, 359.3 × 10^3 km^3/year over ocean precipitation, and 429 × 10^3 km^3/year evaporation. In recent years, Haddeland et al. (2011) compared 11 model simulations for the period 1985-1999 (Table 2). Observation-based data for global precipitation overland had an average value of 126 × 10^3 km^3/year, simulated evapotranspiration, and runoff mean values range between (60 to 85) × 10^3 km^3/year and (42 to 66) × 10^3 km^3/year, respectively. Note that Manabe's evapotranspiration estimate is the only flux within the values reported by Haddeland et al. (2011). Besides, the later estimates are within the range for annual averages reported by Baumgartner and Reichel (1972), hinting that despite the substantial uncertainties and approximations, the values reported in the previous period were not that far from the current ones.

Model simulations did represent a new data source with seeming advantages over observations like the ability to generate global coverage data and perhaps more revolutionary to forecast, predict, and project. Nevertheless, once again, the scientific community relied heavily on observational data because it was crucial for model calibration and validation. Consequently, this novel opportunity to research global water cycle variability and its response to global warming further stressed the need for better observation-based measurements and more accurate quantification of the cycle components.

2.3 Satellite Era

Shortly after the introduction of climate models (Phillips 1956), the Television Infrared Observation Satellite (TIROS-1 or TIROS-A) became the first weather satellite successfully launched in 1960, and so it began the satellite era (NOAA 1987). Barnes and Bowley (1968) proved the effectiveness of satellite observations in hydrology when they published their findings on snow cover mapping over the Missouri and Upper Mississippi River basins. Thereafter, several satellite missions made it into orbit, among the most notable, we may mention the National Aeronautics and Space Administration (NASA) Earth Observing System (EOS) missions. Based on their orbits, satellites could be grouped into two major groups, either geosynchronous orbit (GEO) or polar orbit. Many of the satellites involved in the EOS missions have a nearly polar orbit. Polar-orbit satellites move around the Earth in a Sun-synchronous orbit so that the overpass occurs at the same local time every day, taking around 100 minutes to complete an orbit. These satellites overpass the equator at the same local solar time each day. Satellite sensors could be active or passive, and it is not uncommon for both to be onboard the same satellite. For example, the Tropical Rainfall Measuring Mission (TRMM) Microwave Imager (TMI), a passive sensor, and the Precipitation Radar (PR), an active sensor, were onboard the TRMM satellite. Regarding satellites and missions of particular interest for global water cycle quantification, we have the TRMM (Huffman et al. 2007) and the Global Precipitation Measurement (GPM) (Huffman et al. 2015) for precipitation, the Moderate Resolution Imaging Spectroradiometer (MODIS) for evapotranspiration (Mu et al. 2011), and the Gravity Recovery and Climate Experiment (GRACE) for total water storage (Tapley et al. 2004). There is no specific instrument nor mission dedicated solely to runoff yet (Hong et al. 2007). However, runoff could be derived from other satellite observations, for instance, TRMM precipitation (Huffman et al. 2007), and MODIS land cover (Friedl et al. 2002) using the Natural Resources Conservation Service (NRCS) runoff curve number method (Cronshey 1986; Burges et al. 1998).

Satellite observations complemented the traditional surface measurements and offered unprecedented observational coverage on a global scale (McCabe et al. 2017). The Defense Meteorological Satellite Program (DMSP) near-polar orbiting satellites have been key providers of data over the oceans since 1987 (Dubach and Ng 1988). Onboard their satellites, the most notable instruments are the Special Sensor Microwave Imager (SSM/I) (Hollinger 1991) and its successor, the Special Sensor Microwave Imager Sounder (SSMIS) (Kunkee et al. 2008). These passive microwave radiometers provide measurements used to derive data on surface wind speed, atmospheric water vapor, cloud liquid water, and rain rate, which are critical to quantifying the global water cycle (Robertson et al. 2014). Furthermore, various present-day models and reanalysis products assimilate satellite observations (Van Dijk et al. 2011). Nonetheless, like for GCMs, ground observations are crucial for satellite data validation. Notwithstanding, the number of ground stations worldwide has been declining since the 1970s (Walker et al. 2016). It was not before Trenberth et al. (2007) that the availability of observational and modeled data to quantify the global water cycle was exploited. A year prior, Oki and Kanae (2006) presented a quantitative synthesis of the global water cycle. Instead of estimating the budget, they made a compilation of individual studies to stress the importance of global water cycle quantification and further assessment to manage renewable freshwater resources properly. This concern has been in the minds of the scientific community for quite some time now (Falkenmark and Lindh 1974). The budget assessments by Trenberth et al. and Oki & Kanae are held in high regard and are often used as a sort of validation reference (Rodell et al. 2015).

Oki and Kanae (2006) addressed the availability of renewable freshwater resources for human consumption within the global water cycle. The authors stressed that freshwater availability would be better assessed by fluxes than by storages because water is a circulating resource. Also, given the high variability of the water cycle in time and space, water stress is not a problem of how much water is available but a matter of when and where it is available (Postel et al. 1996). To better represent their research, they synthesized previous estimates of global water cycle fluxes and storages (Korzoun (1978), Shiklomanov (1998), Dirmeyer et al. (2006), and Oki (2006)). By doing so, they also presented a much more comprehensive mean state of the global water cycle. Their results showed overland precipitation of 111×10^3 km^3/year, evapotranspiration of 65.5×10^3 km^3/year, and runoff of 45.5×10^3 km^3/year. Moreover, precipitation is divided into rainfall and snowfall, plus the fluxes are allocated to different terrains or land uses. Over oceans, precipitation was 391×10^3 km^3/year and evaporation was 436.5×10^3 km^3/year.

Trenberth et al. (2007) used different data sources to quantify the global water cycle and its components. Three data sets were selected for precipitation, the Global Precipitation Climatology Project (GPCP v2; Adler et al. 2003), the University of East Anglia Climatic Research Unit time-series (CRU TS 2.1; Mitchell and Jones 2005), and the PRECipitation REConstruction over Land (PREC/L; Chen et al. 2002). Evapotranspiration was simulated using the Community Land Model version 3 (CLM3; Bonan et al. 2002; Qian et al. 2004), which was forced using a combined PREC/L and GPCP precipitation data set. Surface plus subsurface runoff was derived from two climatic water balance estimates (evapotranspiration minus precipitation), the first from the European Centre for Medium Range Weather Forecasts Reanalysis 45 year product (ERA40; Uppala et al. 2005) using the methods described by Trenberth and Guillemot (1998), and the second using evapotranspiration from CLM3 and GPCP precipitation. Additionally, the authors relied on previous work for some components of the global water cycle like surface runoff (Dai and Trenberth 2002), ice volumes (Houghton et al. 2001), soil moisture (Webb et al. 1993), and groundwater (Schlesinger 2005). It was common for prior studies to cite values that, in return, cite another and so on. Unlike them, the authors documented, and traced back as far as possible, the origins of the values used. They reported 113 × 10^3 km^3/year overland precipitation, 73 × 10^3 km^3/year evapotranspiration, 40 × 10^3 km^3/year runoff, 373 × 10^3 km^3/year over ocean precipitation, and 413 × 10^3 km^3/year evaporation.

It is important to note that satellite data records are recently of sufficient time frame lengths and with methods "mature" enough to develop meaningful global water cycle climatology records that can provide information on its components mean state and variability (Schlosser and Houser 2007; Robertson et al. 2014). Exploiting the increasing availability and maturity of satellite products, Sheffield et al. (2009) addressed the feasibility of closing the water budget, relying solely on satellite-based products. They combined the TRMM Multi-satellite Precipitation Analysis (TMPA; Huffman et al. 2007) and the Climate Prediction Center morphing method (CMORPH; Joyce et al. 2004) products for precipitation, the University of Colorado GRACE time series (CSR RL04; Wahr et al. 1998) for total water storage, and they derived evapotranspiration from Aqua satellite data using the Penman-Monteith revised formulation proposed by Mu et al. (2007). Then they evaluated their findings over the Mississippi River basin comparing their runoff estimates, computed as the budget residual, with ground observations. Their results indicate that the data products selected do not close the budget because the computed runoff is greatly overestimated compared to ground measurements. The authors suggest that further improvement of satellite-based products may reduce the residual and suggest multi-source data merging as a complementary means to achieve budget closure.

2.4 Age of Big Data

In this day and age, we have transitioned from minimal data coverage and sources into a widely heterogeneous abundance. In contrast to the continuous decline in the number of ground stations, satellite-based and model-derived data products have proliferated. However, while some components of the global water cycle have multiple products to choose from (e.g., precipitation), others do not (e.g., total water storage). Some products assimilate or calibrate against ground station data to improve their performance (Rudolf and Schneider 2005); others implemented machine learning processing to do so (Hong et al. 2004). It is not uncommon to find performance comparisons between products in the literature, evincing large differences in the magnitude and the variability of the estimates (e.g., as much as 300 mm/year difference between precipitation data sets; Sun et al. 2018). In their global comparison of 30 data sets at multiple spatiotemporal scales, Sun et al. (2018) found that, in general, variability from reanalysis data sets is more substantial than that from other data sources. Conversely, we can see that no single data set performs the best in all regions and at all scales. Aware of that fact, some studies did not look for the best individual data set, but the best combination of data sets towards budget closure of the water cycle over one (Azarderakhsh et al. 2011) or multiple basins (Lorenz et al. 2014). It should be pointed out that the above studies' success metric was not budget closure itself, but validation versus in situ runoff instead.

The paradigm of quantifying the global water cycle is steadily shifting from identifying the best data source per water cycle component into developing the best way to merge data from various sources to complement each other. Various integration methodologies have emerged, among the most widely used ones are: Bayesian model averaging, constrained linear regression, neural networks, optimal interpolation, and simple weighting (Bishop 1995; Hoeting et al. 1999; Rodgers 2000; Aires et al. 2004). Also, post-processing closure methodologies, which distributed the budget residual R among the components based on each component's uncertainties, explored Monte Carlo applications and Kalman filter variations (Pan and Wood 2006; Munier and Aires 2018). Specifics vary from method to method, but, in general, combining different data sets consists of three steps. These steps are an initial assessment of the products to be combined, followed by the integration of the products, and finally, budget closure post-processing.

Data integration is not a new concept nor the methods mentioned above, but its implementation altogether with closure constraints into the quantification of the water cycle is. Sahoo et al. (2011) used 16 data sets (eight for precipitation, six for evapotranspiration, one for runoff, and one for total water storage) applying simple weighting integration over ten basins across the globe, determining water cycle budget non-closure between $5-25\%$. Likewise, Pan et al. (2012) used eight data sets (four for precipitation, two for evapotranspiration, one for runoff, and one for total water storage) in 32 different basins. The authors focused on describing the uncertainty contribution of each component rather than focusing on budget closure, and found that, in general, most of the closure error comes from evapotranspiration.

To date, only a few studies have adopted multi-source data integration at the global scale (Rodell et al. 2015; Zhang et al. 2016; Munier and Aires 2018). The differences between studies and their results reside either on the data sets selected or in the post-processing. Rodell et al. (2015), using six data sets (one for precipitation, three for evapotranspiration, one for runoff, and one for total water storage; Table 3), reported a non-closure residual of less than 10%. The authors adopted the variational data assimilation algorithm of L'Ecuyer and Stephens (2002) and adjusted it to optimize the global water cycle budget closure at the annual scale. They reported $(116.5 \pm 5.1) \times 10^3$ km^3/year overland precipitation, $(70.6 \pm 5.0) \times 10^3$ km^3/year evapotranspiration, $(45.9 \pm 4.4) \times 10^3$ km^3/year runoff, $(403.5 \pm 22.2) \times 10^3$ km^3/year over ocean precipitation, and $(449.5 \pm 22.2) \times 10^3$ km^3/year evaporation. Note that the estimates reported by Oki and Kanae (2006) and Trenberth et al. (2011) lie within the above findings with the only two exceptions of overland precipitation from Oki and Kanae (2006) and runoff from Trenberth et al. (2011).

Zhang et al. (2016), using 14 data sets (five for precipitation, six for evapotranspiration, one for runoff, and two for total water storage; Table 4), assessed the effect of different data sources in the estimation of the water cycle and its budget closure. By removing/replacing in situ observations, reanalysis products, model simulations, or satellite products before data integration, the authors observed that removing non-satellite sources worsens

Table 3 Compiled from Rodell et al. (2015). *P* is precipitation, ET is evapotranspiration, *Q* is runoff, and *Δ*TWS is changes in total water storage

Data source	Variable	Reference(s)
GPCP v2.2	*P*	Adler et al. (2003); Huffman et al. (2009)
Princeton ET	ET	Vinukollu et al. (2011b)
MERRA and MERRA-Land	ET	Rienecker et al. (2011); Bosilovich et al. (2011); Reichle (2012)
GLDAS	ET	Rodell et al. (2004)
University of Washington runoff	*Q*	Clark et al. (2015)
CSR RL05	*Δ*TWS	Chambers and Bonin (2012); Johnson and Chambers (2013); Tapley et al. (2004)

Table 4 Modified from Zhang et al. (2016). *P* is precipitation, ET is evapotranspiration, *Q* is runoff, and TWS is total water storage

Data source	Variable	Reference(s)
CSU	*P*	Bytheway and Kummerow (2013)
PGF	*P*	Sheffield et al. (2006)
CHIRPS	*P*	Funk et al. (2014)
GPCC(v6)	*P*	Schneider et al. (2014)
TMPA-RT	*P*	Huffman et al. (2007), (2010)
SRB-PGF-PM	ET	Vinukollu et al. (2011a)
VIC	ET	Sheffield and Wood (2007)
ERA-interim	ET	Simmons (2006)
MERRA	ET	Rienecker et al. (2011)
GLEAM	ET	Gonzalez Miralles et al. (2011)
SRB-CFSR-SEBS	ET	Vinukollu et al. (2011a)
SRB-CFSR-PM	ET	Vinukollu et al. (2011a)
SRB-CFSR-PT	ET	Vinukollu et al. (2011a)
VIC	*Q*	Sheffield and Wood (2007)
VIC	TWS	Sheffield and Wood (2007)
GRACE	TWS	Landerer and Swenson (2012)

closure errors. Furthermore, as for satellite data sets, they indicate that budget closure error depends on the use of satellite-only data sets or satellite-gauge combined data sets. Regardless of the combination of data sets, the budget could not be closed and, thus, a constrained Kalman filter was used, as developed by Sahoo et al. (2011). They reported a non-closure residual that ranges between $7.6 - 10.4\%$ when using satellite products that lack gauge-based corrections, which is reduced to $4.2 - 9.0\%$ when using gauge-corrected satellite products.

Munier and Aires (2018) integrated 12 data sets (four for precipitation, three for evapotranspiration, one for runoff, and four for total water storage; Table 5) over 11 basins to test a budget closure correction model. The authors define the Calibration Index for Closure (CIC), which depends on the values of precipitation minus evapotranspiration (P − ET) and the Normalized Difference Vegetation Index (NDVI), and based on the CIC values,

Table 5 Modified from Munier and Aires (2018). *P* is precipitation, ET is evapotranspiration, *Q* is runoff, and ΔTWS is total water storage change

Data source	Variable	Reference(s)
TMPA	*P*	Huffman et al. (2007)
CMORPH	*P*	Joyce et al. (2004)
NRL	*P*	Turk et al. (2010)
GPCP	*P*	Adler et al. (2003)
GLEAM	ET	Gonzalez Miralles et al. (2011)
MOD16	ET	Mu et al. (2007)
NTSG	ET	Zhang et al. (2010)
GRDC	*Q*	http://www.grdc.sr.unh.edu/
CSR	ΔTWS	http://www2.csr.utexas.edu/grace/
GFZ	ΔTWS	ftp://isdcftp.gfz-potsdam.de/grace/
JPL	ΔTWS	https://grace.jpl.nasa.gov/data/get-data/
GRGS	ΔTWS	https://grace.obs-mip.fr/

assigned the basins into one of four classes. Then the closure correction model is calibrated to each basin using the corresponding CIC class, and it optimizes budget closure for the fluxes one at the time. While no absolute values are reported, the authors describe how this novel method reduced non-closure residuals by 26% of the value it would have using constrained Kalman filter post-processing.

In the above-mentioned studies, there is a methodological consensus to use simple weighting when integrating data from various sources. This is in good agreement with Aires (2014) who compared the performance of different integration methods, and reported that simple weighting is the most suitable one. Simple weighting offers a straightforward formulation, and more elaborate methods do not offer enough improvement on results to justify the increased complexity they carry along. The assumption for the simple weighting method is that the errors associated with the different products are Gaussian (zero-mean) and independent. However, there might be cases that this assumption may not hold, especially for gauge-based data products, and the dependence among products will cause an underestimation of the error associated with the integrated data set. The combined data set for a given component of the global water cycle (*P*, ET, *Q*, or *Δ*TWS) is equal to:

$$x = \sum_{i=1}^{n} w_i x_i \tag{4}$$

where x is the combined data set for the single component of the global water cycle being integrated, x_1, x_2, x_3, ..., x_n are the different products considered, w_i is the associated weight of product x_i and is defined as:

$$w_i = \frac{\left(\bar{x} - x_i\right)^{-2}}{\sum_{j=1}^{n} \left(\bar{x} - x_j\right)^{-2}} \tag{5}$$

where $\bar{x}$ is the arithmetic mean of the n data products considered, and $\left(\bar{x} - x_i\right)^2$ is defined as the error variance. That is to say, the weight associated to each product is proportional to the inverse of its error variance. Finally, the error associated to the combined data set x is:

$$e_x = \frac{1}{\sum_{i=1}^{n} \left(\bar{x} - x_i\right)^{-2}} \tag{6}$$

3 Status Quo et Verisimile Futurum

It might have been noticed that the chronology of global water cycle quantification does not follow a linear timeline. The epochs started at different points in time without replacing the one before. Each epoch did not only continue to develop, but just like global water cycle components, they interacted with each other in a feedback loop. A convergence point is the fact that model simulations and satellite-based measurements depend upon ground observations either for validation or calibration. The latest epoch, the age of big data, does not intend to merge all the previous into one, but to exploit the various data sources stemming from them to generate the most accurate estimates possible. Therefore, we should keep working on the continuous improvement of ground measurements, model simulations, and satellite observations, which will inherently improve their integration. Abbott et al. (2019) provided one of the most recent descriptions of the global water cycle. Analogously to

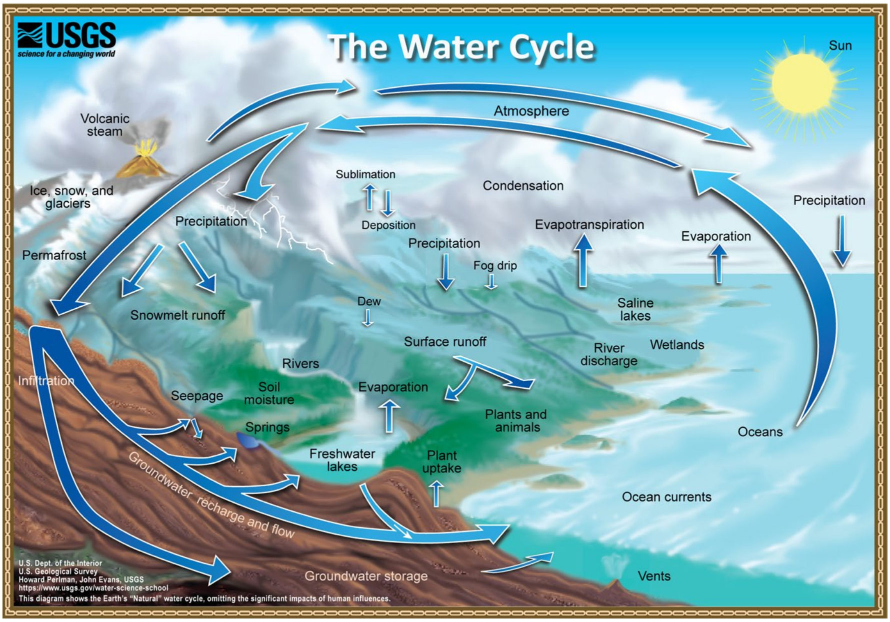

Fig. 3 The Water Cycle. Credit: Howard Perlman, United States Geological Survey (USGS)

Oki and Kanae (2006), the authors did not quantify the global water cycle components themselves but synthesized data from the literature. The authors did not aim to quantify the components of the global water cycle but to assess its correct representation. To do so, they compiled over 464 diagrams (e.g., Fig. 3) and estimates from over 80 studies. Human interaction was absent in approximately 85% of the diagrams, highlighting the omission of the non-negligible anthropogenic component of the water cycle. In addition, the authors stress the necessity to represent seasonal and interannual variability of the global water cycle fluxes and storages in diagrams because the general understanding of temporal variability of the global water cycle is absent in the collective consciousness (Cardak 2009). Within the studies, not all of them reported estimates for all components of the global water cycle. The synthesis resulted in the following estimates: overland precipitation 110×10^3 km^3/year, evapotranspiration 69×10^3 km^3/year, and runoff 46×10^3km^3/year; over oceans, precipitation 380×10^3km^3/year and evaporation 420×10^3 km^3/year.

Herein, building upon the previous compendium done by Baumgartner and Reichel (1972), we surveyed the recent literature, and to the best of our knowledge, compiled all the different estimates of global water cycle components available in peer review journals that at least report the average annual fluxes for the terrestrial or oceanic water cycle (Table 6). Since 2010 it has become more common for studies to address only the terrestrial water cycle (e.g., Van der Ent et al. 2010; Haddeland et al. 2011; Jasechko et al. 2013; Zhang et al. 2018). On the other hand, ocean salinity measurements are being exploited to study the oceanic branch of the water cycle (Durack 2015), yet there are very few studies focusing solely on the oceanic water cycle (e.g., Syed et al. 2010; Robertson et al. 2014; Gutenstein et al. 2021). Inspecting the chronology of global water cycle flux annual average estimates over land and over oceans, it is safe to state that uncertainty estimates associated with fluxes over oceans is higher than that over land (Figs. 4(a) and 4(b)). Comparing

Table 6 All the fluxes are in 10^3 km^3/year. P_L is precipitation overland, ET is evapotranspiration overland, Q is runoff, P_O is precipitation over oceans, E is evaporation over oceans, P_{TOT} is total global precipitation, and E_{TOT} is total global evaporation

Author	P_L	ET	Q	P_O	E	P_{TOT}	E_{TOT}
Manabe (1969)	93.4	69.5	23.9	359.3	429	452.7	498.5
Baumgartner and Reichel (1972)	100	65	35	383	418	483	483
Falkenmark and Lindh (1974)	114	73	41	412	453	526	526
Speidel and Agnew (1982)	111	71	39.7	385	425	496	496
NRC (1986)	107	71	36	398	434	505	505
Van der Leeden (1990)	100	70	39.6	320	350	420	420
Gleick (1993)	119	72	47	458	505	577	577
Schmitt (1995)	110.4	69.4	41	384.7	425.7	495.1	495.1
Shiklomanov (1998)	119	74.2	42.7	458	502.8	577	577
Oki (1999)	115	75	40	391	431	506	506
Oki and Kanae (2006)	111	65.5	45.5	391	436.5	502	502
Schlosser and Houser (2007)	103.5	63	40.5	376	417	479.5	480
Trenberth et al. (2007)	113	73	40	373	413	486	486
Lim and Roderick (2009)	113	78.8	34.1	417.7	451.8	530.7	530.8
Syed et al. (2010)			36.1	374.2	409.2		
Van der Ent et al. (2010)	117	82	35				
Chapin III et al. (2011)	110	71	40	385	425	495	496
Haddeland et al. (2011)	126	72.5	54				
Trenberth et al. (2011)	114	74	40	386	426	500	500
Jasechko et al. (2013)	110	72.7	37.3				
Durack (2015)	110.4	85.1	39.4	384.7	410	495.1	495.1
Rodell et al. (2015)	116.5	70.6	45.9	403.5	449.5	520	520.1
Schneider et al. (2017)	117.6	71.8	45.8	386	431.8	503.6	503.6
Zhang et al. (2018)	114.7	68	46.6				
Abbott et al. (2019)	110	69	46	380	420	490	489

the standard deviation and the interquartile range of the estimates from Oki (1999) onward with the ones from all the estimates (1905-2019), we can affirm that variability has diminished in recent years (Figs. 4(c) and 4(d)). Moreover, the variability of ocean precipitation and evaporation was reduced by more than 70%. These findings advocate that the consistency of the estimates has been improved.

Despite our survey compiling estimates available in the literature rather than presenting a more "traditional" estimates' time series, we observe an increasing trend in the global water cycle fluxes annual average as the year of publication progresses (Fig. 5). We should remark that the years listed correspond to the publication date and do not necessarily reflect on the data sets' reference period used by the authors therein. Hence, our observations are of qualitative and not quantitative character. An increasing trend in global water cycle fluxes, commonly referred to as intensification, is often attributed to global warming; however, the processes that drive the global water cycle's response are yet to be fully understood (Allan et al. 2020). Take note that these estimates are global and do not describe changes in the water cycle at different smaller scales. On top of that, we should not assess these results conclusively because most studies used different data sources and different

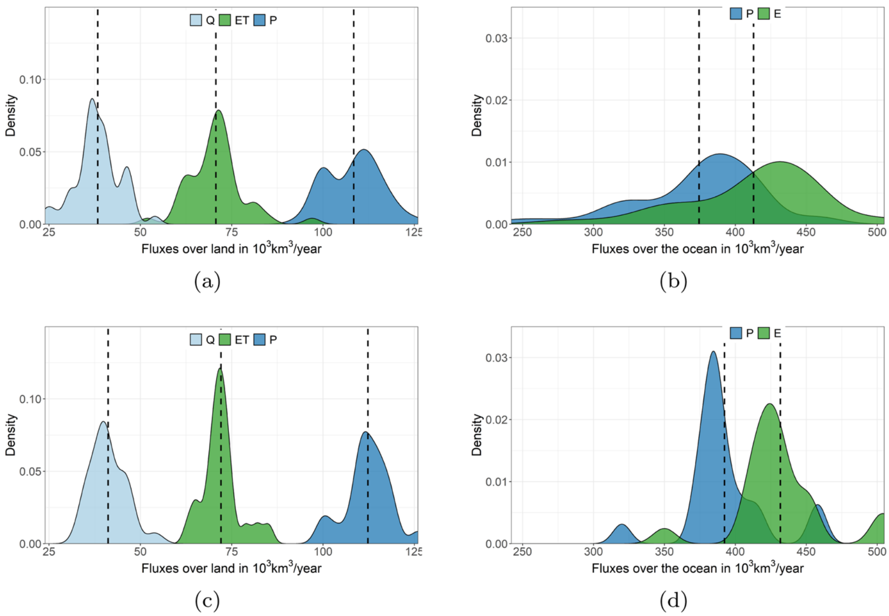

Fig. 4 Probability density distribution of global water cycle fluxes from Tables 1 and 6. The dashed line represents the mean value of each flux. (a) Overland fluxes where *P* is precipitation, ET is evapotranspiration, and *Q* is runoff. (b) Over ocean fluxes where *P* is precipitation and *E* is evaporation. (c) Same as (a) but only for Table 6. (d) same as (b) but only for Table 6

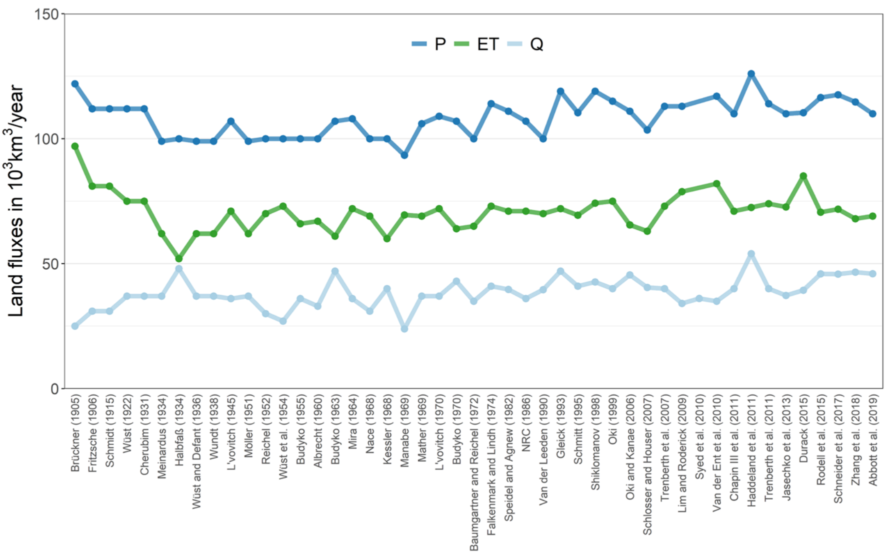

Fig. 5 Chronological estimates of global water cycle fluxes over land in 10^3 km^3/year. *P* is precipitation, ET is evapotranspiration, and *Q* is runoff. The years listed correspond to the publication date and do not necessarily reflect the data sets' reference period used by the authors

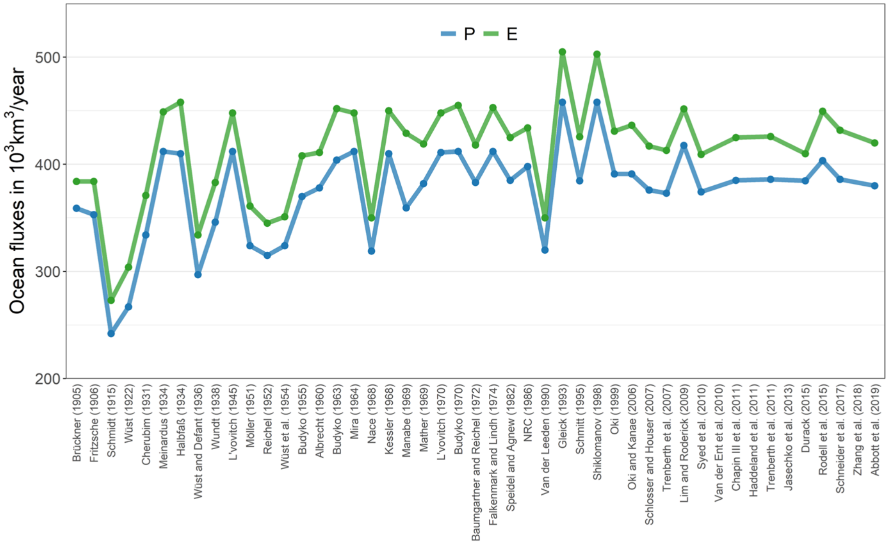

Fig. 6 Chronological estimates of global water cycle fluxes over oceans in 10^3 km^3/year. *P* is precipitation and *E* is evaporation. The years listed correspond to the publication date and do not necessarily reflect the data sets' reference period used by the authors

methods at different development stages, as discussed in the previous section. For example, if we were to look only at Table 6 entries in Fig. 6 (from Baumgartner and Reichel (1972) onward), we would not be able to clearly discriminate a trend from the variability present

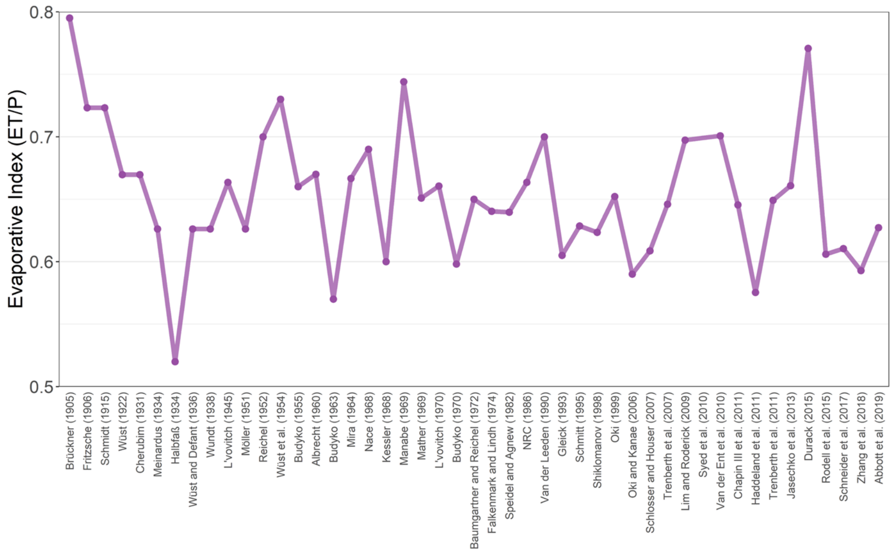

Fig. 7 Chronological estimates of the evaporative index. This is defined as the ratio between evapotranspiration and precipitation overland (ET/*P*). The years listed correspond to the publication date and do not necessarily reflect the data sets' reference period used by the authors

in those estimates. Moreover, suppose we were to omit the estimates reported between Van der Leeden (1990) and Shiklomanov (1998), there seem to be minor oscillations around an overall flat trend, attesting the narrative is dependent on the data being observed. Latch onto the ratio between evapotranspiration and precipitation over land, also known as the Evaporative Index (ET/*P*; Fig. 7), and it is interesting to see how, despite some clear multi-annual oscillations, there seems to be no sharp trend. The Evaporative Index is the fraction of available water consumed by evapotranspiration (Budyko 1974), and assuming no significant change in total water storage, its residual (1− ET/*P*) could be inferred as the fraction that turns into available freshwater. This, at least on paper, would suggest global freshwater availability has not diminished on average.

Through the previous sections, we have described how our understanding of the global water cycle has been evolving over the years as we exploit novel technologies and methods to quantify the components of the global water cycle more accurately. Accordingly, to assess future changes in the global water cycle and its response to global warming, we should study both past shifts documented in observational records and possible changes predicted by model simulations. While there are inherent fluctuations in the global water cycle, some of them are driven by natural phenomena like variations in the Sun and volcanic eruptions (e.g., the year without a summer; Stommel and Stommel 1979), and anthropogenic activities. The latter exerts a continuously increasing influence directly via interference with land surface and water consumption, and indirectly via greenhouse gases and aerosols emissions (Abbott et al. 2019). The nature of the driver and the spatial scale they exercise domain over alter key water cycle characteristics, e.g., precipitation frequency, intensity, or duration (Pendergrass and Hartmann 2014).

Concurrently, model simulations predicted that global mean precipitation would rise in response to CO_2 doubling (Mitchell et al. 1987). The relationship between climate and water cycle caught the attention of both climatic and hydrological communities (Chahine 1992b; Loaiciga et al. 1996). Models and the relationship between climate and water cycle are continuously evaluated in the Assessment Reports of the Intergovernmental Panel on Climate Change (IPCC; Collins et al. 2013; Flato et al. 2014). The Clausius–Clapeyron expression for the saturation vapor pressure establishes that at temperatures typical of the lower troposphere, the water holding capacity increases by about 7% for each 1K increase in temperature. It is safe to assume that an increase in lower-tropospheric water vapor will lead to a chain reaction affecting the entire global water cycle. The poorly understood response of the global water cycle resulted in two main hypotheses: the "changing character of precipitation" and the "dry gets drier, wet gets wetter". The former shows that the increase in global mean precipitation will be unevenly distributed in precipitation events (Trenberth et al. 2003). Heavy or extreme rainfall will become more frequent, while light or moderate precipitation will decline. The latter suggests that the increased vertical gradient of atmospheric water vapor would offset atmospheric wind convergence in the tropics making wet regions wetter and dry regions drier (Roderick et al. 2014). Both hypotheses are today under vigorous debate (Held and Soden 2006; Seager et al. 2010; O'Gorman and Muller 2010; Greve et al. 2014; Roderick et al. 2014; Byrne and O'Gorman 2015; Kumar et al. 2015; Salzmann 2016; Skliris et al. 2016; Wang et al. 2017; Markonis et al. 2019; Allan et al. 2020).

Global precipitation and evapotranspiration, however, are further associated with Earth's energy budget rather than the Clausius-Clapeyron equation (O'Gorman et al. , 2012; Roderick et al. , 2014). Model simulations report that in response to global warming, global precipitation and evapotranspiration, independently of climate forcing, would increase constrained by Earth's energy budget to an expected rate between 2-3%/K (Samset et al. 2018).

Precipitation's response to global warming, also known as apparent hydrological sensitivity, comprises a fast reaction proportional to radiative forcings and a slow temperature-dependent response to the radiative forcings (Bala et al. 2010). Across multiple model simulations, precipitation increases with global warming are generally suppressed over land compared to the global mean (0.8-2.4%/K vs. 2.3-2.7%/K), a behavior partly expected due to limitations on moisture convergence product of the more significant warming over land than oceans (Richardson et al. 2018). Considering that global precipitation's response to global warming is slower than the response of atmospheric water vapor, atmospheric water vapor lifetime must increase to reconcile these different response rates (Hodnebrog et al. 2019). By doing so, regional characteristics of precipitation such as seasonal duration, frequency, and intensity are altered (Pendergrass 2018).

As atmospheric water vapor content increases and its lifetime prolongs, the increased horizontal moisture transport induces an intensification of precipitation minus evapotranspiration patterns. Over the continents, precipitation minus evapotranspiration is positive and accounts for the freshwater flux from the atmosphere to the surface, whereas over the ocean, precipitation minus evaporation is negative and represents the freshwater flux from the oceans to the atmosphere. In dry regions, where evapotranspiration is constrained by water availability, changes in precipitation minus evapotranspiration will be mainly credited to precipitation changes (Roderick et al. 2014). Precipitation minus evapotranspiration over land can be negative during dry seasons or extended drought periods (Kumar et al. 2015). Given that evapotranspiration is a compound flux of evaporation and transpiration, the response of vegetation to global warming and increased CO_2 concentrations in the atmosphere will also determine the characteristics of regional precipitation minus evapotranspiration patterns. Besides, over land, we cannot neglect anthropogenic activities like irrigation, land-use change, deforestation, urbanization, and water withdrawals, among others that directly alter precipitation minus evapotranspiration regimes. On this account, we can expect several factors like topography, atmospheric circulation, anthropogenic tampering, and vegetation response to generate different and complex water cycle responses to global warming.

4 Discussion and Conclusions

Early attempts to quantify the global water cycle date back to the early 1900s (Brückner 1905). To date, despite tremendous advances in terms of data and technology, accuracy regarding the components of the global water cycle has not increased accordingly. Ultimately, unquantified uncertainties on remote sensing satellite products (Sheffield et al. 2009), limitations of climate model simulations (Trenberth et al. 2011), short and heterogeneous observational data records (Schneider et al. 2017), and the natural fluctuations of water cycle components Markonis et al. (2018) keep the understanding of the global water cycle ambiguous and human contribution unattributed. Within the twenty-first century, the paradigm of quantifying the global water cycle has been shifting from identifying the best data source per water cycle component into developing the best way to integrate data from various sources (Aires 2014). Therefore, proper statistical tools for uncertainty quantification (Papalexiou 2018), robust downscaling/disaggregation (Papalexiou et al. 2018), along with analysis over multiple scales (Hanel et al. 2017; Markonis et al. 2021) are required.

The quest for accurate global water cycle quantification gave birth to the Global Energy and Water Exchanges (GEWEX) project. The GEWEX project, formerly known as the

Global Energy and Water Cycle Experiment, started in 1990 and is dedicated to studying the Earth's water and energy cycles (Chahine 1992a). GEWEX established a channel for international research collaboration through different panels, meetings, and projects. Among the most renowned outcomes, we could mention the work of Trenberth et al. (2007), which we further discussed in Sect. 2.3. Speaking of data sets and modeling improvements, GEWEX overlooks eight continental-scale experiments, GEWEX Americas Prediction Project (GAPP; Lawford 1999), Baltic Sea Experiment (BALTEX; Raschke et al. 1998, 2001), GEWEX Asian Monsoon Experiment (GAME; Yasunari 1994), Large Scale Biosphere Atmosphere Experiment in Amazonia (LBA; Marengo 2005), Mackenzie GEWEX Study (MAGS; Stewart et al. 1998), La Plata Basin (LPB; Cavalcanti et al. 2015), The African Monsoon Multidisciplinary Analysis (AMMA; Redelsperger et al. 2006), and Murray-Darling Basin (MDB; Evans and McCabe 2010). Other than the logistic and political criteria, these sites were selected in order to collect data from different climate regimes to assess the global water cycle in a representative manner. The collaborative effort of the international teams involved improved the understanding of regional water balance and feedback processes. The data resulting from the continental-scale experiments are publicly available. Thus, they indirectly started to set up a scientific framework to quantify the global water cycle and close its budget; the latter was obtained within a 10% non-closure tolerance.

As a rule of thumb, ground observations are regarded as the closest measurements to the actual values. However, it is evident that ground observations suffer from systematic errors, mainly because of different environmental and meteorological conditions. For example, the precipitation phase, evaporation from the gauge, and wind drift induce precipitation undercatch on rain gauges (Fuchs et al. 2001). The scientific community is aware that good quality ground observations data represent a cornerstone to quantify the global water cycle, yet we are still unable to deploy a homogeneously distributed global network. Spatial coverage of the Global Precipitation Climatology Centre (GPCC), currently the most comprehensive gauge network available, represents only about 1% of the Earth's surface (assuming no overlap of a 5 km radius per gauge) (Kidd et al. 2017). One of the main reasons behind the struggle to deploy a comprehensive network is that ground stations, and ergo observational data records, are extremely geopolitically dependent (Kibler et al. 2014). In addition, deploying dense monitoring networks unavoidably imply high operational and maintenance costs and spatial requirements (Saltikoff et al. 2017). Consequently, in many developing countries, ground observational records, if available, tend to have multiple temporal discontinuities or non-standardized data quality check protocols (Walker et al. 2016). Different techniques have been used to fill spatiotemporal gaps in observational records. Reconstructing these time series could be achieved using several tools that could be grouped in the following, self-contained infilling (Kemp et al. 1983; Pappas et al. 2014), spatial interpolation (Shepard 1968; Young 1992; Eischeid et al. 1995, 2000), quantile mapping (Simolo et al. 2010; Newman et al. 2015, 2019; Devi et al. 2019), and machine learning methods (Dastorani et al. 2010; Wambua et al. 2016). On a different front, there is an opportunity to use data from amateur networks and the internet of things (i.e., big data with large uncertainty) to enhance spatial coverage and spatiotemporal resolution of traditional ground stations via crowdsourcing and the internet. Needless to say, appropriate validation and quality control procedures must be adopted and implemented to fully exploit the potential to provide a valuable source of high spatiotemporal resolution real-time data (Muller et al. 2015). As of now, however, the lack of adequate ground-based data and station networks still hampers our ability to monitor the water cycle robustly.

Model simulations can generate past climate, current climate, and climate projections data. Moreover, they are capable to switch anthropogenic forcing on precipitation on and off, while the decoupling of natural and anthropogenic forcing remains a challenge on observational data (Allen and Ingram 2002). However, compared to observational data, various characteristics of global water cycle fluxes, and precipitation, in particular, hold uncertainty (Prein and Pendergrass 2019). The simulated projections' temporal length appears to influence precipitation trends, e.g., variability in precipitation estimates are indistinguishable from the noise of internal variability in 20-year or longer runs (Hawkins et al. 2016). Specifications differ from model to model, but in general, recycling of moisture is too large, and the lifetime of moisture is too short across most models, inducing premature precipitation (Trenberth et al. 2011). Also, inaccurate convective parameterizations evidenced that models overestimate precipitation frequency and underestimate its intensity (Trenberth et al. 2017). Analysis focusing on convective precipitation highlighted that its model representation is strongly dependent on the model depiction of cloud microphysics and cloud spatiotemporal variability (Zhao et al. 2016). There is a threefold spread in mean precipitation change with global temperature ($1-3\%\ K^{-1}$), and model simulations showed that there is a correlation between an increase in precipitation extremes and an increase in model resolution, precipitation extremes at the same time showed an anticorrelation with changes in light-moderate precipitation (Thackeray et al. 2018). Furthermore, both the spread and magnitude of change in extreme precipitation vastly exceed those of mean precipitation ($4-10\%\ K^{-1}$) (Kharin et al. 2013). Last but not least, despite the known link between the energy and water global cycles, solar dimming and brightening (the effect of aerosols) are not well represented or sometimes not even considered at all in models; thus, model simulations fail to reproduce variability in the global water cycle intensity (Wild and Liepert 2010).

Satellite remote sensing observations, like models, are limited by their design. Both the orbit they follow and the instrument type (i.e., active or passive) influence global water cycle components' monitoring. The satellite's orbit would delimit its spatiotemporal resolution or coverage. In general, a satellite with high spatial resolution comes with coarse temporal resolution and vice-versa, and high spatiotemporal resolution comes with limited coverage. It has been shown that estimates from active sensors can considerably vary from passive sensor ones, yet they complement each other (Petković and Kummerow 2017). In addition, similarly to ground observations, satellite remote sensing has to deal with different meteorological conditions. For instance, satellite-based global water cycle estimates accuracy is affected by cloud-top reflectance and thermal radiance, making uncertainty larger during the winter or in dry climates (Kummerow et al. 2004). While satellites can monitor the water cycle at the global scale and cover regions inaccessible by ground stations, they still have to tackle the problems involved in complex topography regions. In some cases, the relative biases reach as much as 300% for precipitation estimates (Fekete et al. 2004). Further complications arise from the unique spatiotemporal characteristics of different remotely sensed global water cycle components, making it impossible to assess the water budget without some sort of prior downscaling or integration (Sheffield et al. 2018). E.g., TMPA's precipitation at 25 km every three hours (Huffman et al. 2007), MODIS' evapotranspiration at 1 km daily (Mu et al. 2007), and GRACE's total water storage at $\sim$ 500 km every 30 days(Tapley et al. 2004). Despite all the issues mentioned above, satellite products continue to be the most widely used sources to monitor global water cycle components due to their comprehensive spatial coverage.

It is clear that no global water cycle data source is without fail, and in some cases, one data source strengths cover for other weaknesses. It is typical for satellite-based measurements and model simulations to use ground-based data for validation, calibration, and enhancement purposes. Along the same line, model simulations additionally assimilate satellite-based observations for the above plus for reanalysis. In contrast to the top-down estimation approach used in satellite remote sensing, a bottom-up approach, referred to as reverse hydrology, has been recently proposed (Ciabatta et al. 2020). A physically based selection of surface explanatory variables, like soil moisture, vegetation cover, and topography, is expected to preserve process dynamics and interlinkages within data sets that remain unresolved in conventional statistical downscaling bias-correction methods (Wehbe et al. 2020). It is of utmost importance that the research community strives to improve ground observations, model simulations, and satellite remote sensing measurements individually because more accurate and robust individual data sources will subsequently refine the outcome of multi-source integration. Hence, a three-way integration of satellite remote sensing, model reanalysis, and ground-based measurements, as discussed in Sect. 2.4, is widely acknowledged as the current best practice, particularly when leveraging machine learning tools to handle large data sets.

Acknowledgements This work was supported by the Faculty of Environmental Sciences, Czech University of Life Sciences Prague internal Grant 2020B0001 “A multiscale framework for data analysis of global precipitation”. The data compiled herein and the R code for the figures are publicly available at https://github.com/MiRoVaGo/chronology_gwc.

Declarations

Conflict of interest The authors declare that they have no conflict of interest.

References

Abbott BW, Bishop K, Zarnetske JP, Minaudo C, Chapin F, Krause S, Hannah DM, Conner L, Ellison D, Godsey SE et al. (2019) Human domination of the global water cycle absent from depictions and perceptions. Nature Geoscience 12(7), 533–540

Adler RF, Huffman GJ, Chang A, Ferraro R, Xie PP, Janowiak J, Rudolf B, Schneider U, Curtis S, Bolvin D et al. (2003) The version-2 global precipitation climatology project (gpcp) monthly precipitation analysis (1979-present). Journal of hydrometeorology 4(6):1147–1167

Aires F (2014) Combining datasets of satellite-retrieved products part i: Methodology and water budget closure. Journal of Hydrometeorology 15(4): 1677–1691

Aires F, Prigent C, Rossow W (2004) Neural network uncertainty assessment using bayesian statistics with application to remote sensing: 3. network jacobians. Journal of Geophysical Research: Atmospheres 109(D10)

Albrecht F (1960) Jahreskarten des Wärme-und Wasserhaushaltes der Ozeane. Verlag nicht ermittelbar

Alcamo J, Döll P, Henrichs T, Kaspar F, Lehner B, Rösch T, Siebert S (2003) Development and testing of the watergap 2 global model of water use and availability. Hydrological Sciences Journal 48(3), 317–337

Allan R, Barlow M, Byrne MP, Cherchi A, Douville H, Fowler HJ, Gan TY, Pendergrass AG, Rosenfeld D, Swann AL et al. (2020) Advances in understanding large-scale responses of the water cycle to climate change. Annals of the New York Academy of Sciences 1472: 49–75

Allen MR, Ingram WJ (2002) Constraints on future changes in climate and the hydrologic cycle. Nature 419(6903), 228–232

Arnell NW (1999) A simple water balance model for the simulation of streamflow over a large geographic domain. Journal of Hydrology 217(3–4), 314–335

Azarderakhsh M, Rossow WB, Papa F, Norouzi H, Khanbilvardi R (2011) Diagnosing water variations within the amazon basin using satellite data. Journal of Geophysical Research: Atmospheres 116(D24)

Bala G, Caldeira K, Nemani R (2010) Fast versus slow response in climate change: implications for the global hydrological cycle. Climate dynamics 35(2–3):423–434

Balsamo G, Beljaars A, Scipal K, Viterbo P, van den Hurk B, Hirschi M, Betts AK (2009) A revised hydrology for the ecmwf model: Verification from field site to terrestrial water storage and impact in the integrated forecast system. Journal of hydrometeorology 10(3):623–643
Barnes JC, Bowley CJ (1968) Snow cover distribution as mapped from satellite photography. Water Resources Research 4(2), 257–272
Baumgartner A, Reichel E (1972) Preliminary results of new investigations of world's water balance. Applied optics 7:1705–1710
Bengtsson L (2010) The global atmospheric water cycle. Environmental Research Letters 5(2):025202
Bishop CM et al. (1995) Neural networks for pattern recognition. Oxford University Press
Bonan GB, Oleson KW, Vertenstein M, Levis S, Zeng X, Dai Y, Dickinson RE, Yang ZL (2002) The land surface climatology of the community land model coupled to the ncar community climate model. Journal of climate 15(22):3123–3149
Bondeau A, Smith PC, Zaehle S, Schaphoff S, Lucht W, Cramer W, Gerten D, LOTZE-CAMPEN H, Müller C, Reichstein M (2007) Modelling the role of agriculture for the 20th century global terrestrial carbon balance. Global Change Biology 13(3), 679–706
Bosilovich MG, Robertson FR, Chen J (2011) Global energy and water budgets in merra. Journal of Climate 24(22), 5721–5739
Bralower T, Bice D (2012) Module 4: Introduction to general circulation models. In: Earth 103: Earth in the Future, College of Earth and Mineral Science, The Pennsylvania State University, http://creativecommons.org/licenses/by-nc-sa/4.0/
Brocca L, Filippucci P, Hahn S, Ciabatta L, Massari C, Camici S, Schüller L, Bojkov B, Wagner W (2019) Sm2rain-ascat (2007–2018): global daily satellite rainfall data from ascat soil moisture observations. Earth System Science Data 11(4)
Brückner E (1905) Die bilanz des kreislaufs des wassers auf der erde. Geographische Zeitschrift 11(8. H):436–445
Brutsaert W et al. (2005) Hydrology: an introduction. Cambridge University Press
Budyko MI (1955) Teplowoj Balans Zemnoi Poverkhuorti. Glavnaya geofizicheskaya observatoriya
Budyko MI (1961) The heat balance of the earth's surface. Soviet Geography 2(4), 3–13
Budyko MI (1963) Atlas teplovogo balansa zemnogo shara. Glavnaya geofizicheskaya observatoriya
Budyko MI (1970) The water balance of the oceans. In: Symposium on World Water Balance, Gentbrügge, Int. Ass. Scient. Hydrol., vol 1, pp 24–33
Budyko MI (1974) Climate and life. Academic Press, Inc
Burges SJ, Wigmosta MS, Meena JM (1998) Hydrological effects of land-use change in a zero-order catchment. Journal of Hydrologic Engineering 3(2), 86–97
Byrne MP, O'Gorman PA (2015) The response of precipitation minus evapotranspiration to climate warming: Why the "wet-get-wetter, dry-get-drier" ling does not hold over land. Journal of Climate 28(20), 8078–8092
Bytheway JL, Kummerow CD (2013) Inferring the uncertainty of satellite precipitation estimates in data-sparse regions over land. Journal of Geophysical Research: Atmospheres 118(17), 9524–9533
Cardak O et al. (2009) Science students' misconceptions of the water cycle according to their drawings. Journal of Applied Sciences 9(5), 865–873
Carson D (1982) Current parameterizations of land surface processes in atmospheric general circulation models. Land surface processes in atmospheric general circulation models pp 67–108
Cavalcanti I, Carril A, Penalba O, Grimm A, Menéndez C, Sanchez E, Cherchi A, Sörensson A, Robledo F, Rivera J et al. (2015) Precipitation extremes over la plata basin-review and new results from observations and climate simulations. Journal of hydrology 523:211–230
Chahine MT (1992a) Gewex: The global energy and water cycle experiment. Eos, Transactions American Geophysical Union 73(2), 9–14
Chahine MT (1992b) The hydrological cycle and its influence on climate. Nature 359(6394), 373–380
Chambers D, Bonin J (2012) Evaluation of release-05 grace time-variable gravity coefficients over the ocean. Ocean Science 8(5):859
Chapin III FS, Matson PA, Vitousek P (2011) Principles of terrestrial ecosystem ecology. Springer Science & Business Media
Chen M, Xie P, Janowiak JE, Arkin PA (2002) Global land precipitation: A 50-yr monthly analysis based on gauge observations. Journal of Hydrometeorology 3(3), 249–266
Cherubim R (1931) Uber verdunstungsmessung auf see. Ann d Hydrogr u Marit Meteor 59:325
Ciabatta L, Camici S, Massari C, Filippucci P, Hahn S, Wagner W, Brocca L (2020) Soil moisture and precipitation: The sm2rain algorithm for rainfall retrieval from satellite soil moisture. In: Satellite Precipitation Measurement, Springer, pp 1013–1027

Clark EA, Sheffield J, van Vliet MT, Nijssen B, Lettenmaier DP (2015) Continental runoff into the oceans (1950–2008). Journal of Hydrometeorology 16(4), 1502–1520
Collins M, Knutti R, Arblaster J, Dufresne JL, Fichefet T, Friedlingstein P, Gao X, Gutowski WJ, Johns T, Krinner G, et al. (2013) Long-term climate change: projections, commitments and irreversibility. In: Climate Change 2013-The Physical Science Basis: Contribution of Working Group I to the Fifth Assessment Report of the Intergovernmental Panel on Climate Change, Cambridge University Press, pp 1029–1136
Cox P, Betts R, Bunton C, Essery R, Rowntree P, Smith J (1999) The impact of new land surface physics on the gcm simulation of climate and climate sensitivity. Climate Dynamics 15(3), 183–203
Cronshey R (1986) Urban hydrology for small watersheds. Tech. rep., US Dept. of Agriculture, Soil Conservation Service, Engineering Division
Dai A, Trenberth KE (2002) Estimates of freshwater discharge from continents: Latitudinal and seasonal variations. Journal of hydrometeorology 3(6):660–687
Dalton J (1799) Experiments and observations to determine whether the quantity of rain and dew is equal to the quantity of water carried off by the rivers and raised by evaporation: With an enquiry into the origin of springs. The Manchester Literary and Philosophical Society
Dastorani MT, Moghadamnia A, Piri J, Rico-Ramirez M (2010) Application of ann and anfis models for reconstructing missing flow data. Environmental monitoring and assessment 166(1–4):421–434
Devi U, Shekhar MS, Singh GP, Rao NN, Bhatt US (2019) Methodological application of quantile mapping to generate precipitation data over northwest himalaya. International Journal of Climatology 39(7), 3160–3170
de Rosnay P, Polcher J (1998) Modelling root water uptake in a complex land surface scheme coupled to a gcm. Hydrology and Earth System Sciences Discussions
Dickinson RE (1984) Modeling evapotranspiration for three-dimensional global climate models. Climate processes and climate sensitivity 29:58–72
Dirmeyer PA, Gao X, Zhao M, Guo Z, Oki T, Hanasaki N (2006) Gswp-2: Multimodel analysis and implications for our perception of the land surface. Bulletin of the American Meteorological Society 87(10), 1381–1398
Dubach LL, Ng C (1988) Compendium of meteorological space programs, satellites, and experiments
Durack PJ (2015) Ocean salinity and the global water cycle. Oceanography 28(1), 20–31
Eischeid JK, Bruce Baker C, Karl TR, Diaz HF (1995) The quality control of long-term climatological data using objective data analysis. Journal of applied meteorology 34(12):2787–2795
Eischeid JK, Pasteris PA, Diaz HF, Plantico MS, Lott NJ (2000) Creating a serially complete, national daily time series of temperature and precipitation for the western united states. Journal of Applied Meteorology 39(9), 1580–1591
Essery R, Best M, Betts R, Cox PM, Taylor CM (2003) Explicit representation of subgrid heterogeneity in a gcm land surface scheme. Journal of Hydrometeorology 4(3), 530–543
Evans J, McCabe M (2010) Regional climate simulation over australia's murray-darling basin: A multitemporal assessment. Journal of Geophysical Research: Atmospheres 115(D14)
Falkenmark M, Lindh G (1974) How can we cope with the water resources situation by the year 2015? Ambio pp 114–122
Federer C, Vörösmarty C, Fekete B (1996) Intercomparison of methods for calculating potential evaporation in regional and global water balance models. Water Resources Research 32(7), 2315–2321
Fekete BM, Vörösmarty CJ, Roads JO, Willmott CJ (2004) Uncertainties in precipitation and their impacts on runoff estimates. Journal of Climate 17(2), 294–304
Flato G, Marotzke J, Abiodun B, Braconnot P, Chou SC, Collins W, Cox P, Driouech F, Emori S, Eyring V, et al. (2014) Evaluation of climate models. In: Climate change 2013: the physical science basis. Contribution of Working Group I to the Fifth Assessment Report of the Intergovernmental Panel on Climate Change, Cambridge University Press, pp 741–866
Flato GM (2011) Earth system models: an overview. Wiley Interdisciplinary Reviews: Climate Change 2(6), 783–800
Friedl MA, McIver DK, Hodges JC, Zhang XY, Muchoney D, Strahler AH, Woodcock CE, Gopal S, Schneider A, Cooper A et al. (2002) Global land cover mapping from modis: algorithms and early results. Remote sensing of Environment 83(1–2), 287–302
Fritzsche R (1906) Niederschlag, Abfluss und Verdunstung auf den Landflächen der Erde. as (Dresden Druck von W. Baensch)
Fuchs T, Rapp J, Rubel F, Rudolf B (2001) Correction of synoptic precipitation observations due to systematic measuring errors with special regard to precipitation phases. Physics and Chemistry of the Earth, Part B: Hydrology, Oceans and Atmosphere 26(9), 689–693

Funk CC, Peterson PJ, Landsfeld MF, Pedreros DH, Verdin JP, Rowland JD, Romero BE, Husak GJ, Michaelsen JC, Verdin AP et al. (2014) A quasi-global precipitation time series for drought monitoring. US Geological Survey data series 832(4):1–12

Gleick PH (1993) Water in crisis: a guide to the world's fresh water resources. Oxford University Press, New York

Gonzalez Miralles D, Holmes T, De Jeu R, Gash J, Meesters A, Dolman A (2011) Global land-surface evaporation estimated from satellite-based observations. Hydrology and Earth System Sciences pp 453–469

Gosling SN, Arnell NW (2011) Simulating current global river runoff with a global hydrological model: model revisions, validation, and sensitivity analysis. Hydrological Processes 25(7), 1129–1145

Greve P, Orlowsky B, Mueller B, Sheffield J, Reichstein M, Seneviratne SI (2014) Global assessment of trends in wetting and drying over land. Nature geoscience 7(10):716–721

Gutenstein M, Fennig K, Schröder M, Trent T, Bakan S, Roberts JB, Robertson FR (2021) Intercomparison of freshwater fluxes over ocean and investigations into water budget closure. Hydrology and Earth System Sciences 25(1), 121–146

Haddeland I, Clark DB, Franssen W, Ludwig F, Voß F, Arnell NW, Bertrand N, Best M, Folwell S, Gerten D et al. (2011) Multimodel estimate of the global terrestrial water balance: setup and first results. Journal of Hydrometeorology 12(5), 869–884

Hagemann S, Dümenil L (1997) A parametrization of the lateral waterflow for the global scale. Climate dynamics 14(1):17–31

Hagemann S, Gates LD (2003) Improving a subgrid runoff parameterization scheme for climate models by the use of high resolution data derived from satellite observations. Climate Dynamics 21(3–4), 349–359

Halbfaß W (1934) Flohr, ef beitrag zur methode der kartographischen darstellung von wasserkräften. Geographische Zeitschrift 40(10):391

Hanasaki N, Kanae S, Oki T, Masuda K, Motoya K, Shirakawa N, Shen Y, Tanaka K (2008) An integrated model for the assessment of global water resources-part 1: Model description and input meteorological forcing. Hydrology & Earth System Sciences 12(4)

Hanel M, Kožín R, Heřmanovskỳ M, Roub R (2017) An r package for assessment of statistical downscaling methods for hydrological climate change impact studies. Environmental modelling & software 95:22–28

Hawkins E, Smith RS, Gregory JM, Stainforth DA (2016) Irreducible uncertainty in near-term climate projections. Climate Dynamics 46(11–12), 3807–3819

Hegerl GC, Black E, Allan RP, Ingram WJ, Polson D, Trenberth KE, Chadwick RS, Arkin PA, Sarojini BB, Becker A (2018) Challenges in quantifying changes in the global water cycle. Bulletin of the American Meteorological Society 99(1)

Held IM, Soden BJ (2006) Robust responses of the hydrological cycle to global warming. Journal of climate 19(21):5686–5699

Hersbach H, Bell B, Berrisford P, Hirahara S, Horányi A, Muñoz-Sabater J, Nicolas J, Peubey C, Radu R, Schepers D et al. (2020) The era5 global reanalysis. Quarterly Journal of the Royal Meteorological Society 146(730), 1999–2049

Hildebrand PH, Houser P, Schlosser CA (2003) Observing the global water cycle from space. In: 31st International Conference on Radar Meteorology, Citeseer

Hodnebrog Ø, Myhre G, Samset BH, Alterskjær K, Andrews T, Boucher O, Faluvegi G, Fläschner D, Forster PM, Kasoar M et al. (2019) Water vapour adjustments and responses differ between climate drivers. Atmospheric Chemistry and Physics 19(20), 12887–12899

Hoeting JA, Madigan D, Raftery AE, Volinsky CT (1999) Bayesian model averaging: a tutorial. Statistical science pp 382–401

Hollinger J (1991) Dmsp special sensor microwave/imager calibration/validation. Tech. rep, NAVAL RESEARCH LAB WASHINGTON DC

Hong Y, Hsu KL, Sorooshian S, Gao X (2004) Precipitation estimation from remotely sensed imagery using an artificial neural network cloud classification system. Journal of Applied Meteorology 43(12), 1834–1853

Hong Y, Adler RF, Hossain F, Curtis S, Huffman GJ (2007) A first approach to global runoff simulation using satellite rainfall estimation. Water Resources Research 43(8)

Houghton JT, Ding Y, Griggs DJ, Noguer M, van der Linden P, Dai X, Maskell K, Johnson CA (2001) Climate change 2001: The scientific basis. Cambridge University Press p 881

Huffman GJ, Bolvin DT, Nelkin EJ, Wolff DB, Adler RF, Gu G, Hong Y, Bowman KP, Stocker EF (2007) The trmm multisatellite precipitation analysis (tmpa): Quasi-global, multiyear, combined-sensor precipitation estimates at fine scales. Journal of hydrometeorology 8(1):38–55

Huffman GJ, Adler RF, Bolvin DT, Gu G (2009) Improving the global precipitation record: Gpcp version 2.1. Geophysical Research Letters 36(17)
Huffman GJ, Adler RF, Bolvin DT, Nelkin EJ (2010) The trmm multi-satellite precipitation analysis (tmpa). In: Satellite rainfall applications for surface hydrology, Springer, pp 3–22
Huffman GJ, Bolvin DT, Braithwaite D, Hsu K, Joyce R, Xie P, Yoo SH (2015) Nasa global precipitation measurement (gpm) integrated multi-satellite retrievals for gpm (imerg). Algorithm Theoretical Basis Document (ATBD) Version 4:26
Hurrell JW, Holland MM, Gent PR, Ghan S, Kay JE, Kushner PJ, Lamarque JF, Large WG, Lawrence D, Lindsay K et al. (2013) The community earth system model: a framework for collaborative research. Bulletin of the American Meteorological Society 94(9), 1339–1360
Jasechko S, Sharp ZD, Gibson JJ, Birks SJ, Yi Y, Fawcett PJ (2013) Terrestrial water fluxes dominated by transpiration. Nature 496(7445), 347–350
Johnson GC, Chambers DP (2013) Ocean bottom pressure seasonal cycles and decadal trends from grace release-05: Ocean circulation implications. Journal of Geophysical Research: Oceans 118(9), 4228–4240
Joyce RJ, Janowiak JE, Arkin PA, Xie P (2004) Cmorph: A method that produces global precipitation estimates from passive microwave and infrared data at high spatial and temporal resolution. Journal of hydrometeorology 5(3):487–503
Kemp W, Burnell D, Everson D, Thomson A (1983) Estimating missing daily maximum and minimum temperatures. Journal of climate and applied meteorology 22(9):1587–1593
Kessler A (1968) Globalbilanzen von Klimaelementen: ein Beitrag zur allgemeinen Klimatologie der Erde. na
Kharin VV, Zwiers F, Zhang X, Wehner M (2013) Changes in temperature and precipitation extremes in the cmip5 ensemble. Climatic change 119(2):345–357
Kibler KM, Biswas RK, Juarez Lucas AM (2014) Hydrologic data as a human right? equitable access to information as a resource for disaster risk reduction in transboundary river basins. Water policy 16(S2):36–58
Kidd C, Becker A, Huffman GJ, Muller CL, Joe P, Skofronick-Jackson G, Kirschbaum DB (2017) So, how much of the earth's surface is covered by rain gauges? Bulletin of the American Meteorological Society 98(1), 69–78
Koirala S (2010) Explicit representation of groundwater process in a global-scale land surface model to improve hydrological predictions. PhD thesis, University of Tokyo
Korzoun VI (1978) World water balance and water resources of the earth. Studies and Reports in Hydrology 25
Kumar S, Allan RP, Zwiers F, Lawrence DM, Dirmeyer PA (2015) Revisiting trends in wetness and dryness in the presence of internal climate variability and water limitations over land. Geophysical Research Letters 42(24), 10–867
Kummerow C, Poyner P, Berg W, Thomas-Stahle J (2004) The effects of rainfall inhomogeneity on climate variability of rainfall estimated from passive microwave sensors. Journal of Atmospheric and Oceanic Technology 21(4), 624–638
Kunkee DB, Poe GA, Boucher DJ, Swadley SD, Hong Y, Wessel JE, Uliana EA (2008) Design and evaluation of the first special sensor microwave imager/sounder. IEEE Transactions on Geoscience and Remote Sensing 46(4), 863–883
Landerer FW, Swenson S (2012) Accuracy of scaled grace terrestrial water storage estimates. Water resources research 48(4)
Lawford R (1999) A midterm report on the gewex continental-scale international project (gcip). Journal of Geophysical Research: Atmospheres 104(D16), 19279–19292
L'Ecuyer TS, Stephens GL (2002) An estimation-based precipitation retrieval algorithm for attenuating radars. Journal of applied meteorology 41(3):272–285
Levizzani V, Cattani E (2019) Satellite remote sensing of precipitation and the terrestrial water cycle in a changing climate. Remote Sensing 11(19):2301
Liang X, Lettenmaier DP, Wood EF, Burges SJ (1994) A simple hydrologically based model of land surface water and energy fluxes for general circulation models. Journal of Geophysical Research: Atmospheres 99(D7), 14415–14428
Lim WH, Roderick ML (2009) An Atlas on Global Water Cycle: Based on the IPCC AR4 Climate Models. ANU Press
Loaiciga HA, Valdes JB, Vogel R, Garvey J, Schwarz H (1996) Global warming and the hydrologic cycle. Journal of Hydrology 174(1–2), 83–127

Lorenz C, Kunstmann H, Devaraju B, Tourian MJ, Sneeuw N, Riegger J (2014) Large-scale runoff from landmasses: a global assessment of the closure of the hydrological and atmospheric water balances. Journal of Hydrometeorology 15(6), 2111–2139

L'vovitch M (1945) World water regime elements. Sverdlovsk, Moscow, Russia

L'vovitch M (1970) World water balance (general report). In: World water balance: Proceedings of the Reading Symposium, pp 401–415

L'vovitch M (1973) The global water balance. Eos, Transactions American Geophysical Union 54(1), 28–53

Manabe S (1969) Climate and the ocean circulation: I. the atmospheric circulation and the hydrology of the earth's surface. Monthly Weather Review 97(11):739–774

Marcinek J (1964) Der abfluß von den landflächen der erde und seine verteilung auf 5° zonen. PhD thesis, VEB Verlag für Bauwesen

Marengo JA (2005) Characteristics and spatio-temporal variability of the amazon river basin water budget. Climate Dynamics 24(1), 11–22

Markonis Y, Hanel M, Máca P, Kyselỳ J, Cook E (2018) Persistent multi-scale fluctuations shift european hydroclimate to its millennial boundaries. Nature communications 9(1):1–12

Markonis Y, Papalexiou S, Martinkova M, Hanel M (2019) Assessment of water cycle intensification over land using a multisource global gridded precipitation dataset. Journal of Geophysical Research: Atmospheres 124(21), 11175–11187

Markonis Y, Pappas C, Hanel M, Papalexiou SM (2021) A cross-scale framework for integrating multisource data in earth system sciences. Environmental Modelling & Software 139:104997

Mather JR (1962) Average climatic water balance data of the continents: part 1. africa. Publications in Climatology

Mather JR (1963a) Average climatic water balance data of the continents: part 2. asia (excluding u.s.s.r.). Publications in Climatology

Mather JR (1963b) Average climatic water balance data of the continents: part 3. u.s.s.r. Publications in Climatology

Mather JR (1963c) Average climatic water balance data of the continents: part 4. australia, new zeland, and oceania. Publications in Climatology

Mather JR (1964a) Average climatic water balance data of the continents: part 5. europa. Publications in Climatology

Mather JR (1964b) Average climatic water balance data of the continents: part 6. north america (excluding united states). Publications in Climatology

Mather JR (1964c) Average climatic water balance data of the continents: part 7. united states. Publications in Climatology

Mather JR (1965) Average climatic water balance data of the continents: part 8. south america. Publications in Climatology

Mather JR (1969) The average annual water balance of the world. AWRA Symposium

McCabe MF, Rodell M, Alsdorf DE, Miralles DG, Uijlenhoet R, Wagner W, Lucieer A, Houborg R, Verhoest NE, Franz TE et al. (2017) The future of earth observation in hydrology. Hydrology and earth system sciences 21(7):3879

McGuffie K, Henderson-Sellers A (2001) Forty years of numerical climate modelling. International Journal of Climatology: A Journal of the Royal Meteorological Society 21(9), 1067–1109

Meigh J, McKenzie A, Sene K (1999) A grid-based approach to water scarcity estimates for eastern and southern africa. Water Resources Management 13(2), 85–115

Meinardus W (1934) Eine neue niederschlagskarte der erde. Petermanns Geogr Mitt 80:1–4

Mira A (1964) Physical geographical atlas of the world, moscow, russia, 1964. Sovietgeography, Review and Translation 6

Mitchell J, Wilson C, Cunnington W (1987) On co2 climate sensitivity and model dependence of results. Quarterly Journal of the Royal Meteorological Society 113(475), 293–322

Mitchell TD, Jones PD (2005) An improved method of constructing a database of monthly climate observations and associated high-resolution grids. International Journal of Climatology: A Journal of the Royal Meteorological Society 25(6), 693–712

Möller F (1951) Quarterly charts of rainfall for the whole earth. Petermanns Geograph Mitt 95:1–7

Monteith J, Unsworth M (2013) Principles of environmental physics: plants, animals, and the atmosphere. Academic Press

Mu Q, Heinsch FA, Zhao M, Running SW (2007) Development of a global evapotranspiration algorithm based on modis and global meteorology data. Remote sensing of Environment 111(4), 519–536

Mu Q, Zhao M, Running SW (2011) Improvements to a modis global terrestrial evapotranspiration algorithm. Remote Sensing of Environment 115(8), 1781–1800

Muller C, Chapman L, Johnston S, Kidd C, Illingworth S, Foody G, Overeem A, Leigh R (2015) Crowdsourcing for climate and atmospheric sciences: current status and future potential. International Journal of Climatology 35(11), 3185–3203
Munier S, Aires F (2018) A new global method of satellite dataset merging and quality characterization constrained by the terrestrial water budget. Remote Sensing of Environment 205:119–130
Nace RL (1968) Water of the world geological survey
Newman AJ, Clark MP, Craig J, Nijssen B, Wood A, Gutmann E, Mizukami N, Brekke L, Arnold JR (2015) Gridded ensemble precipitation and temperature estimates for the contiguous united states. Journal of Hydrometeorology 16(6), 2481–2500
Newman AJ, Clark MP, Longman RJ, Gilleland E, Giambelluca TW, Arnold JR (2019) Use of daily station observations to produce high-resolution gridded probabilistic precipitation and temperature time series for the hawaiian islands. Journal of Hydrometeorology 20(3), 509–529
NOAA US (1987) Space-based remote sensing of the earth: a report to the Congress. NASA
NRC (1986) Global Change in the Geosphere-Biosphere. National Academy Press
Oki T (1999) 1.2 the global water cycle. Global Energy and Water Cycles 134800000(10)
Oki T (2006) The hydrologic cycles and global circulation. Encyclopedia of hydrological sciences pp 13–22
Oki T, Kanae S (2006) Global hydrological cycles and world water resources. science 313(5790):1068–1072
Otto-Bliesner BL, Brady EC, Fasullo J, Jahn A, Landrum L, Stevenson S, Rosenbloom N, Mai A, Strand G (2016) Climate variability and change since 850 ce: An ensemble approach with the community earth system model. Bulletin of the American Meteorological Society 97(5), 735–754
O'Gorman P, Muller CJ (2010) How closely do changes in surface and column water vapor follow clausius-clapeyron scaling in climate change simulations? Environmental Research Letters 5(2):025207
O'Gorman PA, Allan RP, Byrne MP, Previdi M (2012) Energetic constraints on precipitation under climate change. Surveys in geophysics 33(3–4):585–608
Palissy B (1580) Discours admirables. Martin Le Jeune, Paris
Pan M, Wood EF (2006) Data assimilation for estimating the terrestrial water budget using a constrained ensemble kalman filter. Journal of Hydrometeorology 7(3), 534–547
Pan M, Sahoo AK, Troy TJ, Vinukollu RK, Sheffield J, Wood EF (2012) Multisource estimation of long-term terrestrial water budget for major global river basins. Journal of Climate 25(9), 3191–3206
Papalexiou SM (2018) Unified theory for stochastic modelling of hydroclimatic processes: Preserving marginal distributions, correlation structures, and intermittency. Advances in water resources 115:234–252
Papalexiou SM, Markonis Y, Lombardo F, AghaKouchak A, Foufoula-Georgiou E (2018) Precise temporal disaggregation preserving marginals and correlations (dipmac) for stationary and nonstationary processes. Water Resources Research 54(10), 7435–7458
Pappas C, Papalexiou SM, Koutsoyiannis D (2014) A quick gap filling of missing hydrometeorological data. Journal of Geophysical Research: Atmospheres 119(15), 9290–9300
Pendergrass AG (2018) What precipitation is extreme? Science 360(6393), 1072–1073
Pendergrass AG, Hartmann DL (2014) Two modes of change of the distribution of rain. Journal of Climate 27(22), 8357–8371
Petković V, Kummerow CD (2017) Understanding the sources of satellite passive microwave rainfall retrieval systematic errors over land. Journal of Applied Meteorology and Climatology 56(3), 597–614
Pfister L, Savenije HH, Fenicia F, et al. (2009) Leonardo Da Vinci's water theory: on the origin and fate of water. Iahs Press
Phillips NA (1956) The general circulation of the atmosphere: A numerical experiment. Quarterly Journal of the Royal Meteorological Society 82(352), 123–164
Pollio MV (1648) De architectura, liber octavus. In: Vitruvius (ed) De Architectura, Elsevier, pp 150 – 172
Postel SL, Daily GC, Ehrlich PR (1996) Human appropriation of renewable fresh water. Science 271(5250), 785–788
Prein AF, Pendergrass AG (2019) Can we constrain uncertainty in hydrologic cycle projections? Geophysical Research Letters 46(7), 3911–3916
Qian T, Dai A, Trenberth KE, Oleson KW, (2006) Simulation of global land surface conditions from 1948 to, (2004) part i: Forcing data and evaluations. Journal of Hydrometeorology 7(5), 953–975
Raschke E, Karstens U, Nolte-Holube R, Brandt R, Isemer HJ, Lohmann D, Lobmeyr M, Rockel B, Stuhlmann R (1998) The baltic sea experiment baltex: A brief overview and some selected results of the authors. Surveys in Geophysics 19(1), 1–22
Raschke E, Meywerk J, Warrach K, Andrea U, Bergström S, Beyrich F, Bosveld F, Bumke K, Fortelius C, Graham L et al. (2001) The baltic sea experiment (baltex): a european contribution to the

investigation of the energy and water cycle over a large drainage basin. Bulletin of the American Meteorological Society 82(11), 2389–2414

Rasmussen JL (1970) The atmospheric water balance and the hydrology of large river basins 1. JAWRA Journal of the American Water Resources Association 6(4), 631–639

Redelsperger JL, Thorncroft CD, Diedhiou A, Lebel T, Parker DJ, Polcher J (2006) African monsoon multidisciplinary analysis: An international research project and field campaign. Bulletin of the American Meteorological Society 87(12), 1739–1746

Reichel E (1952) Der stand des verdunstungsproblems. Ber Dt Wetterdienst US-Zone 35:155–172

Reichle R (2012) The merra-land data product (version 1.2). GMAO Off Note 3

Richardson T, Forster P, Andrews T, Boucher O, Faluvegi G, Fläschner D, Hodnebrog Ø, Kasoar M, Kirkevåg A, Lamarque JF et al. (2018) Drivers of precipitation change: An energetic understanding. Journal of climate 31(23):9641–9657

Rienecker MM, Suarez MJ, Gelaro R, Todling R, Bacmeister J, Liu E, Bosilovich MG, Schubert SD, Takacs L, Kim GK et al. (2011) Merra: Nasa's modern-era retrospective analysis for research and applications. Journal of climate 24(14):3624–3648

Robertson F, Bosilovich M, Roberts J, Reichle R, Adler R, Ricciardulli L, Berg W, Huffman G (2014) Consistency of estimated global water cycle variations over the satellite era. Journal of Climate 27(16), 6135–6154

Rodell M, Houser P, Jambor U, Gottschalck J, Mitchell K, Meng CJ, Arsenault K, Cosgrove B, Radakovich J, Bosilovich M et al. (2004) The global land data assimilation system. Bulletin of the American Meteorological Society 85(3), 381–394

Rodell M, Beaudoing HK, L'Ecuyer T, Olson WS, Famiglietti JS, Houser PR, Adler R, Bosilovich MG, Clayson CA, Chambers D et al. (2015) The observed state of the water cycle in the early twenty-first century. Journal of Climate 28(21), 8289–8318

Roderick M, Sun F, Lim WH, Farquhar G (2014) A general framework for understanding the response of the water cycle to global warming over land and ocean. Hydrology and Earth System Sciences 18(5), 1575–1589

Rodgers CD (2000) Inverse methods for atmospheric sounding: theory and practice, vol 2. World scientific

Rost S, Gerten D, Bondeau A, Lucht W, Rohwer J, Schaphoff S (2008) Agricultural green and blue water consumption and its influence on the global water system. Water Resources Research 44(9)

Rudolf B, Schneider U (2005) Calculation of gridded precipitation data for the global land-surface using in-situ gauge observations. In: Proc. Second Workshop of the Int. Precipitation Working Group, pp 231–247

Sahoo AK, Pan M, Troy TJ, Vinukollu RK, Sheffield J, Wood EF (2011) Reconciling the global terrestrial water budget using satellite remote sensing. Remote Sensing of Environment 115(8), 1850–1865

Saltikoff E, Kurri M, Leijnse H, Barbosa S, Stiansen K (2017) Maintenance keeps radars running. Bulletin of the American Meteorological Society 98(9), 1833–1840

Salzmann M (2016) Global warming without global mean precipitation increase? Science advances 2(6):e1501572

Samset BH, Myhre G, Forster P, Hodnebrog Ø, Andrews T, Boucher O, Faluvegi G, Fläschner D, Kasoar M, Kharin V, et al. (2018) Weak hydrological sensitivity to temperature change over land, independent of climate forcing. npj Climate and Atmospheric Science 1(1):1–8

Schlesinger WH (2005) Biogeochemistry, vol 8. Elsevier

Schlosser CA, Houser PR (2007) Assessing a satellite-era perspective of the global water cycle. Journal of climate 20(7):1316–1338

Schmidt W (1915) Strahlung und verdunstung an freien wasserflächen; ein beitrag zum wärmehaushalt des weltmeers und zum wasserhaushalt der erde. Ann Calender Hydrographie und Maritimen Meteorologie 43:111–124

Schmitt RW (1995) The ocean component of the global water cycle. Reviews of Geophysics 33(S2), 1395–1409

Schneider U, Becker A, Finger P, Meyer-Christoffer A, Ziese M, Rudolf B (2014) Gpcc's new land surface precipitation climatology based on quality-controlled in situ data and its role in quantifying the global water cycle. Theoretical and Applied Climatology 115(1–2), 15–40

Schneider U, Finger P, Meyer-Christoffer A, Rustemeier E, Ziese M, Becker A (2017) Evaluating the hydrological cycle over land using the newly-corrected precipitation climatology from the global precipitation climatology centre (gpcc). Atmosphere 8(3):52

Seager R, Naik N, Vecchi GA (2010) Thermodynamic and dynamic mechanisms for large-scale changes in the hydrological cycle in response to global warming. Journal of Climate 23(17), 4651–4668

Sheffield J, Wood EF (2007) Characteristics of global and regional drought, 1950–2000: Analysis of soil moisture data from off-line simulation of the terrestrial hydrologic cycle. Journal of Geophysical Research: Atmospheres 112(D17)

Sheffield J, Goteti G, Wood EF (2006) Development of a 50-year high-resolution global dataset of meteorological forcings for land surface modeling. Journal of climate 19(13):3088–3111

Sheffield J, Ferguson CR, Troy TJ, Wood EF, McCabe MF (2009) Closing the terrestrial water budget from satellite remote sensing. Geophysical Research Letters 36(7)

Sheffield J, Wood EF, Pan M, Beck H, Coccia G, Serrat-Capdevila A, Verbist K (2018) Satellite remote sensing for water resources management: Potential for supporting sustainable development in data-poor regions. Water Resources Research 54(12), 9724–9758

Shepard D (1968) A two-dimensional interpolation function for irregularly-spaced data. In: Proceedings of the 1968 23rd ACM national conference, pp 517–524

Shiklomanov IA (1998) World water resources: A new appraisal and assessment for the 21st century. UNESCO

Shuttleworth WJ, Wallace J (1985) Evaporation from sparse crops-an energy combination theory. Quarterly Journal of the Royal Meteorological Society 111(469), 839–855

Simmons A (2006) Era-interim: New ecmwf reanalysis products from 1989 onwards. ECMWF newsletter 110:25–36

Simolo C, Brunetti M, Maugeri M, Nanni T (2010) Improving estimation of missing values in daily precipitation series by a probability density function-preserving approach. International Journal of Climatology 30(10), 1564–1576

Skliris N, Zika JD, Nurser G, Josey SA, Marsh R (2016) Global water cycle amplifying at less than the clausius-clapeyron rate. Scientific reports 6(1):1–9

Speidel D, Agnew A (1982) The natural geochemistry of our environment. Westview Press p 16

Starr V, Peixoto J (1958) On the global balance of water vapor and the hydrology of deserts. Tellus 10(2), 188–194

Stewart RE, Leighton H, Marsh P, Moore G, Ritchie H, Rouse W, Soulis E, Strong G, Crawford R, Kochtubajda B (1998) The mackenzie gewex study: The water and energy cycles of a major north american river basin. Bulletin of the American Meteorological Society 79(12), 2665–2684

Stommel H, Stommel E (1979) The year without a summer. Scientific American 240(6), 176–187

Sun Q, Miao C, Duan Q, Ashouri H, Sorooshian S, Hsu KL (2018) A review of global precipitation data sets: Data sources, estimation, and intercomparisons. Reviews of Geophysics 56(1), 79–107

Syed TH, Famiglietti JS, Chambers DP, Willis JK, Hilburn K (2010) Satellite-based global-ocean mass balance estimates of interannual variability and emerging trends in continental freshwater discharge. Proceedings of the National Academy of Sciences 107(42), 17916–17921

Takata K, Emori S, Watanabe T (2003) Development of the minimal advanced treatments of surface interaction and runoff. Global and planetary Change 38(1–2), 209–222

Tapiador FJ, Navarro A, Moreno R, Sánchez JL, García-Ortega E (2020) Regional climate models: 30 years of dynamical downscaling. Atmospheric Research 235:104785

Tapley BD, Bettadpur S, Ries JC, Thompson PF, Watkins MM (2004) Grace measurements of mass variability in the earth system. Science 305(5683), 503–505

Thackeray CW, DeAngelis AM, Hall A, Swain DL, Qu X (2018) On the connection between global hydrologic sensitivity and regional wet extremes. Geophysical Research Letters 45(20), 11–343

Thornthwaite CW (1948) An approach toward a rational classification of climate. Geographical review 38(1):55–94

Trenberth KE, Guillemot CJ (1998) Evaluation of the atmospheric moisture and hydrological cycle in the ncep/ncar reanalyses. Climate Dynamics 14(3), 213–231

Trenberth KE, Dai A, Rasmussen RM, Parsons DB (2003) The changing character of precipitation. Bulletin of the American Meteorological Society 84(9), 1205–1218

Trenberth KE, Smith L, Qian T, Dai A, Fasullo J (2007) Estimates of the global water budget and its annual cycle using observational and model data. Journal of Hydrometeorology 8(4), 758–769

Trenberth KE, Fasullo JT, Mackaro J (2011) Atmospheric moisture transports from ocean to land and global energy flows in reanalyses. Journal of climate 24(18):4907–4924

Trenberth KE, Zhang Y, Gehne M (2017) Intermittency in precipitation: Duration, frequency, intensity, and amounts using hourly data. Journal of Hydrometeorology 18(5), 1393–1412

Turk JT, Mostovoy GV, Anantharaj V (2010) The nrl-blend high resolution precipitation product and its application to land surface hydrology. In: Satellite Rainfall Applications for Surface Hydrology, Springer, pp 85–104

Uppala SM, Kållberg P, Simmons A, Andrae U, Bechtold VDC, Fiorino M, Gibson J, Haseler J, Hernandez A, Kelly G et al. (2005) The era-40 re-analysis. Quarterly Journal of the Royal Meteorological

Society: A journal of the atmospheric sciences, applied meteorology and physical oceanography 131(612):2961–3012
Van Dijk A, Renzullo LJ, et al. (2011) Water resource monitoring systems and the role of satellite observations. Copernicus GmbH
Van der Ent RJ, Savenije HH, Schaefli B, Steele-Dunne SC (2010) Origin and fate of atmospheric moisture over continents. Water Resources Research 46(9)
Van der Leeden F (1990) The water encyclopedia. CRC Press
Vinukollu RK, Meynadier R, Sheffield J, Wood EF (2011a) Multi-model, multi-sensor estimates of global evapotranspiration: Climatology, uncertainties and trends. Hydrological Processes 25(26), 3993–4010
Vinukollu RK, Wood EF, Ferguson CR, Fisher JB (2011b) Global estimates of evapotranspiration for climate studies using multi-sensor remote sensing data: Evaluation of three process-based approaches. Remote Sensing of Environment 115(3), 801–823
Wahr J, Molenaar M, Bryan F (1998) Time variability of the earth's gravity field: Hydrological and oceanic effects and their possible detection using grace. Journal of Geophysical Research: Solid Earth 103(B12), 30205–30229
Walker D, Forsythe N, Parkin G, Gowing J (2016) Filling the observational void: Scientific value and quantitative validation of hydrometeorological data from a community-based monitoring programme. Journal of Hydrology 538:713–725
Wambua RM, Mutua BM, Raude JM (2016) Prediction of missing hydro-meteorological data series using artificial neural networks (ann) for upper tana river basin, kenya. vol 4:35–43
Wang G, Wang D, Trenberth KE, Erfanian A, Yu M, Bosilovich MG, Parr DT (2017) The peak structure and future changes of the relationships between extreme precipitation and temperature. Nature Climate Change 7(4), 268–274
Wang K, Dickinson RE (2012) A review of global terrestrial evapotranspiration: Observation, modeling, climatology, and climatic variability. Reviews of Geophysics 50(2)
Webb RS, Rosenzweig CE, Levine ER (1993) Specifying land surface characteristics in general circulation models: Soil profile data set and derived water-holding capacities. Global Biogeochemical Cycles 7(1), 97–108
Wehbe Y, Temimi M, Adler RF (2020) Enhancing precipitation estimates through the fusion of weather radar, satellite retrievals, and surface parameters. Remote Sensing 12(8):1342
Wild M, Liepert B (2010) The earth radiation balance as driver of the global hydrological cycle. Environmental Research Letters 5(2):025203
Willmott CJ, Rowe CM, Mintz Y (1985) Climatology of the terrestrial seasonal water cycle. Journal of Climatology 5(6), 589–606
Willmott CJ, Robeson SM, Feddema JJ (1994) Estimating continental and terrestrial precipitation averages from rain-gauge networks. International Journal of Climatology 14(4), 403–414
Wundt W (1938) Das Bild des Wasserkreislaufs auf Grund früherer und neuer Forschungen. Reichs-und Preuß, Ministerium für Ernährung und Landwirtschaft, Landesanst
Wüst G (1922) Verdunstung und niederschlag auf der erde. Z Ges f Erdkunde Berlin
Wüst G, Defant A (1936) Schichtung und Zirkulation des atlantischen Ozeans. W. de Gruyter
Wüst G, Brogmus W, Noodt E (1954) Die zonale verteilung von salzgehalt, niederschlag, verdunstung, temperatur und dichte an der oberfläche der ozeane. Kieler Meeresforschungen 10(1954):2
Yasunari T (1994) Gewex-related asian monsoon experiment (game). Advances in space research 14(1):161–165
Young KC (1992) A three-way model for interpolating for monthly precipitation values. Monthly Weather Review 120(11), 2561–2569
Zhang K, Kimball JS, Nemani RR, Running SW (2010) A continuous satellite-derived global record of land surface evapotranspiration from 1983 to 2006. Water Resources Research 46(9)
Zhang Y, Pan M, Wood EF (2016) On creating global gridded terrestrial water budget estimates from satellite remote sensing. In: Remote Sensing and Water Resources, Springer, pp 59–78
Zhang Y, Pan M, Sheffield J, Siemann AL, Fisher CK, Liang M, Beck HE, Wanders N, MacCracken RF, Houser PR, et al. (2018) A climate data record (cdr) for the global terrestrial water budget: 1984–2010. Hydrology and Earth System Sciences (Online) 22(PNNL-SA-129750)
Zhao M, Golaz JC, Held IM, Ramaswamy V, Lin SJ, Ming Y, Ginoux P, Wyman B, Donner L, Paynter D et al. (2016) Uncertainty in model climate sensitivity traced to representations of cumulus precipitation microphysics. Journal of Climate 29(2), 543–560